

Conditional moment analysis of steady state unsaturated flow in bounded, randomly heterogeneous soils

Zhiming Lu and Shlomo P. Neuman

Department of Hydrology and Water Resources, University of Arizona, Tucson, Arizona, USA

Alberto Guadagnini

Dipartimento di Ingegneria Idraulica Ambientale e del Rilevamento, Politecnico di Milano, Milan, Italy

Daniel M. Tartakovsky

Los Alamos National Laboratory, Los Alamos, New Mexico, USA

Received 27 September 2000; revised 21 September 2001; accepted 21 September 2001; published 26 April 2002.

[1] We consider steady state unsaturated flow in bounded, randomly heterogeneous soils under the influence of random boundary and source terms. Our aim is to predict pressure heads and fluxes without resorting to Monte Carlo simulation, upscaling, or linearization of the constitutive relationship between unsaturated hydraulic conductivity and pressure head. We represent this relationship through Gardner's exponential model while treating its exponent α as a random constant and saturated hydraulic conductivity K_s as a spatially correlated random field. We linearize the steady state unsaturated flow equations by means of the Kirchhoff transformation and integrate them in probability space to obtain exact integro-differential equations for the conditional mean and variance-covariance of transformed pressure head and flux. After approximating these equations recursively to second order in the standard deviation σ_Y of $Y = \ln K_s$, we solve them by finite elements for superimposed mean uniform and divergent flows in the vertical plane, with and without conditioning on measured Y values. Comparison with Monte Carlo solutions demonstrates that whereas our nonlocal solution is nominally restricted to mildly nonuniform media with $\sigma_Y^2 \ll 1$, it yields remarkably accurate results for strongly nonuniform media with σ_Y^2 at least as large as 2. This accords well with a previous theoretical analysis, which shows that the solution may remain asymptotic for values of σ_Y^2 as large as 2. *INDEX TERMS:* 1866 Hydrology: Soil moisture; 1869 Hydrology: Stochastic processes; 1875 Hydrology: Unsaturated zone; 3210 Mathematical Geophysics: Modeling; *KEYWORDS:* unsaturated flow, heterogeneity, randomness, conditioning, uncertainty

1. Introduction

[2] Saturated hydraulic conductivity and the parameters of constitutive relations between relative conductivity and pressure head in unsaturated soils vary spatially in a manner that cannot be described with certainty. Therefore they are often modeled as correlated random fields, rendering the corresponding unsaturated flow equations stochastic. If the (geo)statistical properties of these fields can be inferred from measurements, the stochastic flow equations can be solved numerically by conditional Monte Carlo simulation. The corresponding first moments constitute optimum unbiased predictors of quantities such as pressure head and flux. Conditional second moments constitute measures of associated prediction errors.

[3] The Monte Carlo method is conceptually straightforward and has the advantage of applying to a very broad range of both linear and nonlinear flow and transport problems. A major conceptual disadvantage of the Monte Carlo approach is that it provides no theoretical insight into the nature of the solution. There additionally is neither a theory to tell whether or not and at what rate should one expect a particular Monte Carlo solution to converge to its exact (ensemble) solution, nor are there well-established computational criteria to reliably terminate the Monte

Carlo process at a given level of accuracy. This is especially true about second (joint) moments (not to speak of higher moments or the probability distribution) of Monte Carlo results. On a more pragmatic level, the Monte Carlo approach tends to be computationally intensive by requiring numerous simulations to yield statistically meaningful samples and a fine computational grid to resolve high-frequency random fluctuations. Hence there are strong theoretical and pragmatic reasons to pursue alternative computational approaches, which are capable of predicting as accurately and efficiently as possible flow and transport in randomly nonuniform media.

[4] We consider a deterministic alternative to conditional Monte Carlo simulation which allows predicting steady state unsaturated flow under uncertainty and assess the latter without having to generate random fields or variables, without upscaling, and without linearizing the constitutive characteristics of the soil. Neuman *et al.* [1999] and Tartakovsky *et al.* [1999] have shown that such prediction is possible when soil properties scale according to the linearly separable model of Vogel *et al.* [1991]. They have demonstrated that when the scaling parameter of pressure head is a random variable independent of location, the steady state unsaturated flow equations can be linearized by means of the Kirchhoff transformation for gravity-free flow. Linearization is also possible in the presence of gravity when hydraulic conductivity varies exponentially with pressure head according to the exponential model of Gardner [1958]. By treating the exponent α in

Gardner's model as a random constant and the log saturated hydraulic conductivity $Y = \ln K_s$ as a random field, *Tartakovsky et al.* [1999] were able to develop exact conditional first- and second-moment equations for unsaturated flow, which are nonlocal (integro-differential) and therefore non-Darcian. A survey of the literature by these authors concerning the spatial variability of α has revealed that treating it as a random constant, rather than as a spatially varying random field, may be a minor disadvantage in comparison to the advantage of preserving nonlinearity in the constitutive relationship between hydraulic conductivity and pressure head.

[5] Though the conditional moment equations are mathematically exact, they nevertheless require a closure approximation to be workable. *Tartakovsky et al.* [1999] developed recursive approximations for these equations to second order in the standard deviations of Y , σ_Y , and zero order in the standard deviations of $\beta = \ln \alpha$, σ_β as well as the forcing terms. They solved them analytically for the mean Kirchhoff potential, pressure head, and corresponding variances under one-dimensional vertical infiltration, without conditioning. Upon comparing these with Monte Carlo results obtained by solving the stochastic Richards equation numerically, the authors found that second-order approximations are generally far superior to zero-order approximations, and the variance of pressure heads compares much better with Monte Carlo values than does the variance of Kirchhoff potentials. Both the analytical pressure head and its variances compared well with Monte Carlo results for input variances at least as large as 1. This accorded well with their theoretical analysis, which had shown that the analytical solution remains asymptotic for input variances as large as 2.

[6] *Tartakovsky et al.* [1999] were able to show rigorously that the concept of effective or equivalent hydraulic conductivity does not generally apply to statistically averaged, Kirchhoff-transformed unsaturated flow equations, except when they are unconditional and flow is driven solely by gravity. In fact, all quantities that enter into their conditional moment equations are defined on a unique support scale ω , which obviates the need for upscaling (i.e., eliminates the need for introducing effective or equivalent hydraulic parameters defined over volumes larger than ω).

[7] The conditional moment equations of *Tartakovsky et al.* [1999] are exact, provided forcing terms are known with certainty. In this study we extend them to account more fully for uncertain forcing terms. Elsewhere [*Lu*, 2000], we have approximated these equations recursively to second order in the standard deviations σ_Y of $Y = \ln K_s$, σ_β of $\beta = \ln \alpha$, and those of forcing terms (on the assumption that these random variables are mutually uncorrelated) and formulated a corresponding finite element algorithm in two dimensions. As we have implemented this algorithm only to zero order in σ_β and the forcing terms, we limit our discussion here to this latter case. The corresponding recursive conditional moment equations are similar to those of *Tartakovsky et al.* [1999]. We discretize them by finite elements in a way reminiscent of that done by *Guadagnini and Neuman* [1999a] for saturated flow. We then implement our algorithm in the vertical plane under superimposed mean uniform and divergent flows, with and without conditioning on measured Y values. We present computational results and assess their accuracy through comparison with Monte Carlo solutions of Richards' equation. Whereas our nonlocal solution is nominally restricted to mildly nonuniform media with $\sigma_Y^2 \ll 1$, we find that it actually yields remarkably accurate results for strongly nonuniform media with σ_Y^2 at least as large as 2. This accords well with a theoretical

analysis by *Tartakovsky et al.* [1999], which shows that the solution may remain asymptotic for values of σ_Y^2 as large as 2.

2. Statement of Problem

[8] We describe steady state unsaturated flow by means of Darcy's law

$$\mathbf{q}(\mathbf{x}) = -K(\mathbf{x}, \psi) \nabla [\psi(\mathbf{x}) + gx_3] \quad \mathbf{x} \text{ in } \Omega \quad (1)$$

and the continuity equation

$$-\nabla \cdot \mathbf{q}(\mathbf{x}) + f(\mathbf{x}) = 0 \quad \mathbf{x} \text{ in } \Omega \quad (2)$$

subject to the boundary conditions

$$\psi(\mathbf{x}) = \Psi(\mathbf{x}) \quad \mathbf{x} \text{ on } \Gamma_D \quad (3)$$

$$-\mathbf{q}(\mathbf{x}) \cdot \mathbf{n}(\mathbf{x}) = Q(\mathbf{x}) \quad \mathbf{x} \text{ on } \Gamma_N, \quad (4)$$

where \mathbf{q} is volumetric Darcy flux, K is unsaturated hydraulic conductivity, ψ is pressure head, g is 1 for flow with gravity and 0 for gravity-free flow, x_3 is the vertical coordinate, f is a random source term, Ψ is a randomly prescribed pressure head on the Dirichlet boundary Γ_D , Q is a randomly prescribed flux into the flow domain Ω across the Neumann boundary Γ_N , and \mathbf{n} is a unit vector outward normal to the boundary Γ of Ω . All quantities in equations (1), (2), (3), and (4) are defined on a support volume ω , centered about point \mathbf{x} , which is small compared to Ω but large enough to render the quantities measurable and the equations locally valid [*Neuman and Orr*, 1993; *Tartakovsky et al.*, 1999]. This operational definition of ω does not generally conform to a representative elementary volume (REV) in the traditional sense [*Bear*, 1972]. We take the random forcing terms f , Ψ , and Q to be prescribed in a statistically independent manner. Substituting equation (1) into equation (2) yields the stochastic steady state Richards' equation

$$\nabla \cdot [K(\mathbf{x}, \psi) \nabla (\psi(\mathbf{x}) + gx_3)] + f(\mathbf{x}) = 0 \quad \mathbf{x} \text{ in } \Omega. \quad (5)$$

We write the unsaturated hydraulic conductivity as

$$K(\mathbf{x}, \psi) = K_s(\mathbf{x}) K_r(\mathbf{x}, \psi), \quad (6)$$

where the saturated conductivity K_s is a random field and the relative conductivity K_r is given by *Gardner's* [1958] exponential model

$$K_r(\mathbf{x}, \psi) = e^{\alpha\psi(\mathbf{x})}. \quad (7)$$

[9] On the basis of considerations presented by *Tartakovsky et al.* [1999] we treat α as a space-independent random constant. This allows us to define the Kirchhoff transformation

$$\Phi(\mathbf{x}) = \int_{-\infty}^{\psi(\mathbf{x})} K_r(\xi) d\xi = \frac{1}{\alpha} e^{\alpha\psi(\mathbf{x})}, \quad (8)$$

which transforms equation (5) and the boundary condition equations (3) and (4), respectively, into

$$\nabla \cdot [K_s(\mathbf{x})(\nabla\Phi(\mathbf{x}) + g\alpha\Phi(\mathbf{x})\mathbf{e}_3)] + f(\mathbf{x}) = 0 \quad \mathbf{x} \text{ in } \Omega \quad (9)$$

$$\Phi(\mathbf{x}) = H(\mathbf{x}) \quad H(\mathbf{x}) = \frac{1}{\alpha} e^{\alpha\Psi(\mathbf{x})} \quad \mathbf{x} \text{ on } \Gamma_D \quad (10)$$

$$\mathbf{n}(\mathbf{x}) \cdot [K_s(\mathbf{x})(\nabla\Phi(\mathbf{x}) + g\alpha\Phi(\mathbf{x})\mathbf{e}_3)] = Q(\mathbf{x}) \quad \mathbf{x} \text{ on } \Gamma_N, \quad (11)$$

where $\mathbf{e}_3 = (0, 0, 1)^T$ is a unit vector and T denotes transpose.

3. Exact Conditional Moment Equations

[10] We express saturated hydraulic conductivity as

$$K_s(\mathbf{x}) = \langle K_s(\mathbf{x}) \rangle + K'_s(\mathbf{x}) \quad \langle K'_s(\mathbf{x}) \rangle \equiv 0, \quad (12)$$

where $\langle \cdot \rangle$ signifies conditional ensemble mean and prime denotes (generally nonhomogeneous) random fluctuations about this mean. As such, $\langle K_s(\mathbf{x}) \rangle$ represents a relatively smooth unbiased estimate of the unknown random function $K_s(\mathbf{x})$, conditioned on measurements at discrete points in space. If the measurements consist of K_s values, then the conditional spatial statistics of K_s (or, more commonly, its natural logarithm $Y = \ln K_s$) can be determined (in principle) by geostatistical methods such as kriging. Likewise, we write

$$\Phi(\mathbf{x}) = \langle \Phi(\mathbf{x}) \rangle + \Phi'(\mathbf{x}) \quad \langle \Phi'(\mathbf{x}) \rangle \equiv 0 \quad (13)$$

$$\alpha = \langle \alpha \rangle + \alpha' \quad \langle \alpha' \rangle \equiv 0. \quad (14)$$

3.1. Exact Conditional Mean Equations

[11] Substituting equations (12), (13), and (14) into equation (9), (10), and (11) and taking conditional ensemble mean yield the following exact conditional mean equations for the Kirchhoff-transformed variable Φ ,

$$\nabla \cdot [\langle K_s(\mathbf{x}) \rangle \nabla \langle \Phi(\mathbf{x}) \rangle - \mathbf{r}(\mathbf{x}) + g(\langle \alpha \rangle \langle K_s(\mathbf{x}) \rangle \langle \Phi(\mathbf{x}) \rangle + \langle \alpha \rangle R_{K\Phi}(\mathbf{x}) + \langle K_s(\mathbf{x}) \rangle R_{\alpha\Phi}(\mathbf{x}) + R_{\alpha K\Phi}(\mathbf{x})) \mathbf{e}_3] + \langle f(\mathbf{x}) \rangle = 0 \quad \mathbf{x} \text{ in } \Omega \quad (15)$$

$$\langle \Phi(\mathbf{x}) \rangle = \langle H(\mathbf{x}) \rangle \quad \mathbf{x} \text{ on } \Gamma_D \quad (16)$$

$$\mathbf{n}(\mathbf{x}) \cdot [\langle K_s(\mathbf{x}) \rangle \nabla \langle \Phi(\mathbf{x}) \rangle - \mathbf{r}(\mathbf{x}) + g(\langle \alpha \rangle \langle K_s(\mathbf{x}) \rangle \langle \Phi(\mathbf{x}) \rangle + \langle \alpha \rangle R_{K\Phi}(\mathbf{x}) + \langle K_s(\mathbf{x}) \rangle R_{\alpha\Phi}(\mathbf{x}) + R_{\alpha K\Phi}(\mathbf{x})) \mathbf{e}_3] = \langle Q(\mathbf{x}) \rangle \quad \mathbf{x} \text{ on } \Gamma_N. \quad (17)$$

[12] In Appendix A, we develop an exact explicit expression for the conditional mean flux,

$$\langle \mathbf{q}(\mathbf{x}) \rangle = -\langle K_s(\mathbf{x}) \rangle [\nabla \langle \Phi(\mathbf{x}) \rangle + g\langle K_s(\mathbf{x}) \rangle (\langle \alpha \rangle \langle \Phi(\mathbf{x}) \rangle + R_{\alpha\Phi}(\mathbf{x})) \mathbf{e}_3] + \mathbf{r}(\mathbf{x}) - g(\langle \alpha \rangle R_{K\Phi}(\mathbf{x}) + R_{\alpha K\Phi}(\mathbf{x})) \mathbf{e}_3 \quad (18)$$

and show that

$$\begin{aligned} \mathbf{r}(\mathbf{x}) &\equiv -\langle K'_s(\mathbf{x}) \nabla \Phi'(\mathbf{x}) \rangle = \int_{\Omega} \langle K'_s(\mathbf{x}) \nabla_x \nabla_x^T G(\mathbf{z}, \mathbf{x}) K'_s(\mathbf{z}) \rangle \\ &\cdot [\nabla \langle \Phi(\mathbf{z}) \rangle + g\langle \alpha \rangle \langle \Phi(\mathbf{z}) \rangle \mathbf{e}_3] d\Omega + \int_{\Omega} \langle K'_s(\mathbf{x}) \nabla_x \nabla_x^T G(\mathbf{z}, \mathbf{x}) \rangle \\ &\cdot \mathbf{r}(\mathbf{z}) d\Omega + g \int_{\Omega} \langle \alpha' K'_s(\mathbf{x}) \nabla_x \nabla_x^T G(\mathbf{z}, \mathbf{x}) K_s(\mathbf{z}) \rangle \langle \Phi(\mathbf{z}) \rangle \mathbf{e}_3 d\Omega \\ &- g \int_{\Omega} \langle K'_s(\mathbf{x}) \nabla_x \nabla_x^T G(\mathbf{z}, \mathbf{x}) \rangle (\langle \alpha \rangle R_{K\Phi}(\mathbf{z}) + \langle K_s(\mathbf{z}) \rangle R_{\alpha\Phi}(\mathbf{z}) \\ &+ R_{\alpha K\Phi}(\mathbf{z})) \mathbf{e}_3 d\Omega + \int_{\Gamma_D} \langle K'_s(\mathbf{x}) H'(\mathbf{z}) \nabla_x \nabla_x^T G(\mathbf{z}, \mathbf{x}) K_s(\mathbf{z}) \rangle \\ &\cdot \mathbf{n}(\mathbf{z}) d\Gamma \end{aligned} \quad (19)$$

$$\begin{aligned} R_{K\Phi}(\mathbf{x}) &\equiv \langle K'_s(\mathbf{x}) \Phi'(\mathbf{x}) \rangle = - \int_{\Omega} \langle K'_s(\mathbf{x}) \nabla_x^T G(\mathbf{z}, \mathbf{x}) K'_s(\mathbf{z}) \rangle \\ &\cdot [\nabla \langle \Phi(\mathbf{z}) \rangle + g\langle \alpha \rangle \langle \Phi(\mathbf{z}) \rangle \mathbf{e}_3] d\Omega - \int_{\Omega} \langle K'_s(\mathbf{x}) \nabla_x^T G(\mathbf{z}, \mathbf{x}) \rangle \\ &\cdot \mathbf{r}(\mathbf{z}) d\Omega - g \int_{\Omega} \langle \alpha' K'_s(\mathbf{x}) \nabla_x^T G(\mathbf{z}, \mathbf{x}) K_s(\mathbf{z}) \rangle \langle \Phi(\mathbf{z}) \rangle \mathbf{e}_3 d\Omega \\ &+ g \int_{\Omega} \langle K'_s(\mathbf{x}) \nabla_x^T G(\mathbf{z}, \mathbf{x}) \rangle (\langle \alpha \rangle R_{K\Phi}(\mathbf{z}) + \langle K_s(\mathbf{z}) \rangle R_{\alpha\Phi}(\mathbf{z}) \\ &+ R_{\alpha K\Phi}(\mathbf{z})) \mathbf{e}_3 d\Omega - \int_{\Gamma_D} \langle K'_s(\mathbf{x}) H'(\mathbf{z}) \nabla_x^T G(\mathbf{z}, \mathbf{x}) K_s(\mathbf{z}) \rangle \\ &\cdot \mathbf{n}(\mathbf{z}) d\Gamma \end{aligned} \quad (20)$$

$$\begin{aligned} R_{\alpha\Phi}(\mathbf{x}) &\equiv \langle \alpha' \Phi'(\mathbf{x}) \rangle = - \int_{\Omega} \langle \alpha' \nabla_x^T G(\mathbf{z}, \mathbf{x}) K'_s(\mathbf{z}) \rangle \\ &\cdot [\nabla \langle \Phi(\mathbf{z}) \rangle + g\langle \alpha \rangle \langle \Phi(\mathbf{z}) \rangle \mathbf{e}_3] d\Omega - \int_{\Omega} \langle \alpha' \nabla_x^T G(\mathbf{z}, \mathbf{x}) \rangle \\ &\cdot \mathbf{r}(\mathbf{z}) d\Omega - g \int_{\Omega} \langle \alpha'^2 \nabla_x^T G(\mathbf{z}, \mathbf{x}) K_s(\mathbf{z}) \rangle \langle \Phi(\mathbf{z}) \rangle \mathbf{e}_3 d\Omega \\ &+ g \int_{\Omega} \langle \alpha' \nabla_x^T G(\mathbf{z}, \mathbf{x}) \rangle (\langle \alpha \rangle R_{K\Phi}(\mathbf{z}) + \langle K_s(\mathbf{z}) \rangle R_{\alpha\Phi}(\mathbf{z}) \\ &+ R_{\alpha K\Phi}(\mathbf{z})) \mathbf{e}_3 d\Omega - \int_{\Gamma_D} \langle \alpha' H'(\mathbf{z}) \nabla_x^T G(\mathbf{z}, \mathbf{x}) K_s(\mathbf{z}) \rangle \\ &\cdot \mathbf{n}(\mathbf{z}) d\Gamma \end{aligned} \quad (21)$$

$$\begin{aligned} R_{\alpha K\Phi}(\mathbf{x}) &\equiv \langle \alpha' K'_s(\mathbf{x}) \Phi'(\mathbf{x}) \rangle = - \int_{\Omega} \langle \alpha' K'_s(\mathbf{x}) \nabla_x^T G(\mathbf{z}, \mathbf{x}) K'_s(\mathbf{z}) \rangle \\ &\cdot [\nabla \langle \Phi(\mathbf{z}) \rangle + g\langle \alpha \rangle \langle \Phi(\mathbf{z}) \rangle \mathbf{e}_3] d\Omega - \int_{\Omega} \langle \alpha' K'_s(\mathbf{x}) \nabla_x^T G(\mathbf{z}, \mathbf{x}) \rangle \\ &\cdot \mathbf{r}(\mathbf{z}) d\Omega - g \int_{\Omega} \langle \alpha'^2 K'_s(\mathbf{x}) \nabla_x^T G(\mathbf{z}, \mathbf{x}) K_s(\mathbf{z}) \rangle \langle \Phi(\mathbf{z}) \rangle \mathbf{e}_3 d\Omega \\ &+ g \int_{\Omega} \langle \alpha' K'_s(\mathbf{x}) \nabla_x^T G(\mathbf{z}, \mathbf{x}) \rangle (\langle \alpha \rangle R_{K\Phi}(\mathbf{z}) + \langle K_s(\mathbf{z}) \rangle R_{\alpha\Phi}(\mathbf{z}) \\ &+ R_{\alpha K\Phi}(\mathbf{z})) \mathbf{e}_3 d\Omega - \int_{\Gamma_D} \langle \alpha' K'_s(\mathbf{x}) H'(\mathbf{z}) \nabla_x^T G(\mathbf{z}, \mathbf{x}) K_s(\mathbf{z}) \rangle \\ &\cdot \mathbf{n}(\mathbf{z}) d\Gamma, \end{aligned} \quad (22)$$

where G is an auxiliary random function defined in Appendix A.

[13] We note that equations (18) and (19) of *Tartakovsky et al.* [1999] for \mathbf{r} , $R_{K\Phi}$ and $R_{\alpha\Phi}$, which correspond to our equations (19), (20), and (21), do not include integrals over Γ_D . Even in the special case where Ψ on Γ_D in equation (3) is deterministic, its Kirchhoff transform H is not deterministic unless α is also deterministic. It follows that equations (18) and (19) of *Tartakovsky et al.* [1999] are valid only when both Ψ and α are deterministic.

3.2. Exact Conditional Second Moment Equations

[14] An equation for the conditional covariance function $C_{\Phi}(\mathbf{x}, \mathbf{y}) = \langle \Phi'(\mathbf{x}) \Phi'(\mathbf{y}) \rangle$ of Φ can be obtained upon multiplying equation (A8) in Appendix A by $\Phi'(\mathbf{y})$ and taking conditional ensemble mean,

$$\nabla_x \cdot \mathbf{F}(\mathbf{x}, \mathbf{y}) + \langle f'(\mathbf{x}) \Phi'(\mathbf{y}) \rangle = 0 \quad \mathbf{x} \text{ in } \Omega, \quad \mathbf{y} \text{ in } \Omega \quad (23)$$

$$C_{\Phi}(\mathbf{x}, \mathbf{y}) = \langle H'(\mathbf{x}) \Phi'(\mathbf{y}) \rangle \quad \mathbf{x} \text{ on } \Gamma_D, \quad \mathbf{y} \text{ in } \Omega \quad (24)$$

$$\mathbf{n}(\mathbf{x}) \cdot \mathbf{F}(\mathbf{x}, \mathbf{y}) = \langle Q'(\mathbf{x}) \Phi'(\mathbf{y}) \rangle \quad \mathbf{x} \text{ on } \Gamma_N, \quad \mathbf{y} \text{ in } \Omega \quad (25)$$

$$\begin{aligned}
\mathbf{F}(\mathbf{x}, \mathbf{y}) = & \langle K_s(\mathbf{x}) \rangle \nabla_{\mathbf{x}} C_{\Phi}(\mathbf{x}, \mathbf{y}) + \langle K'_s(\mathbf{x}) \Phi'(\mathbf{y}) \rangle \nabla \Phi'(\mathbf{x}) \\
& + \langle K'_s(\mathbf{x}) \Phi'(\mathbf{y}) \rangle \nabla \langle \Phi(\mathbf{x}) \rangle + g(\langle \alpha \rangle \langle K_s(\mathbf{x}) \rangle C_{\Phi}(\mathbf{x}, \mathbf{y})) \\
& + \langle \alpha \rangle \langle K'_s(\mathbf{x}) \Phi'(\mathbf{x}) \Phi'(\mathbf{y}) \rangle + \langle \alpha' K'_s(\mathbf{x}) \Phi'(\mathbf{x}) \Phi'(\mathbf{y}) \rangle \\
& + \langle K_s(\mathbf{x}) \rangle \langle \alpha' \Phi'(\mathbf{x}) \Phi'(\mathbf{y}) \rangle + \langle K_s(\mathbf{x}) \rangle R_{\alpha\Phi}(\mathbf{y}) \langle \Phi(\mathbf{x}) \rangle \\
& + \langle \alpha' K'(\mathbf{x}) \Phi'(\mathbf{y}) \rangle \langle \Phi(\mathbf{x}) \rangle + \langle \alpha \rangle C_{K\Phi}(\mathbf{x}, \mathbf{y}) \langle \Phi(\mathbf{x}) \rangle \mathbf{e}_3, \quad (26)
\end{aligned}$$

where $C_{K\Phi}(\mathbf{x}, \mathbf{y}) = \langle K'(\mathbf{x}) \Phi'(\mathbf{y}) \rangle$. Expressing Φ' in equation (A8) in terms of \mathbf{y} , multiplying by $f'(\mathbf{x})$ and $Q'(\mathbf{x})$, respectively, then taking conditional ensemble mean yields the source and Neumann boundary moments

$$\langle f'(\mathbf{x}) \Phi'(\mathbf{y}) \rangle = \int_{\Omega} \langle f'(\mathbf{x}) f'(\mathbf{z}) \rangle \langle G(\mathbf{z}, \mathbf{y}) \rangle d\Omega \quad (27)$$

$$\langle Q'(\mathbf{x}) \Phi'(\mathbf{y}) \rangle = \int_{\Gamma_N} \langle Q'(\mathbf{x}) Q'(\mathbf{z}) \rangle \langle G(\mathbf{z}, \mathbf{y}) \rangle d\Gamma. \quad (28)$$

[15] Expressing Φ' in equation (A8) in terms of \mathbf{y} , multiplying by $H'(\mathbf{x})$, and taking conditional ensemble mean would not lead to an expression similar to equation (27) or (28). This is so because in contrast to f and Q , each of which is prescribed in a statistically independent manner, H depends on α , as does G . Therefore one cannot separate the moments of H and G as was done in equation (27) for f and G or in equation (28) for Q and G . It follows that the moment $\langle H'(\mathbf{x}) \Phi'(\mathbf{y}) \rangle$ cannot be simplified in a compact manner without approximation. Suffice it to say that $\langle H'(\mathbf{x}) \Phi'(\mathbf{y}) \rangle$ as well as equations (27) and (28) is generally nonzero, and so equations (23), (24), (25), and (26) include nonhomogeneous source and boundary terms. As such, they are more general than the homogeneous equations (A7), (A8), and (A9) of *Tartakovsky et al.* [1999], which are valid only for deterministic α and forcing terms. The detailed derivation for $\langle H'(\mathbf{x}) \Phi'(\mathbf{y}) \rangle$ is given by *Lu* [2000].

[16] Conditional moments of two or three quantities in equation (26), such as $\langle K'_s(\mathbf{x}) \Phi'(\mathbf{y}) \rangle$ or $\langle K'_s(\mathbf{x}) \Phi'(\mathbf{y}) \nabla \Phi'(\mathbf{x}) \rangle$, cannot be simplified in a compact manner without approximation. Exact expressions for the conditional covariance tensor of flux are obtained upon multiplying equation (A10) by $\mathbf{q}^T(\mathbf{y})$ and taking ensemble mean.

4. Recursive Conditional Moment Approximations

[17] To render the above conditional moment equations workable, it is necessary to employ a suitable closure approximation. *Tartakovsky et al.* [1999] developed recursive approximations for these equations to second order in the standard deviation of Y , σ_Y , and zero order in the standard deviation of $\beta = \ln \alpha$, σ_{β} , as well as forcing terms. Elsewhere [Lu, 2000], we developed recursive approximations on the basis of the above conditional moment equations to second order in both σ_Y and σ_{β} , which account fully for uncertainty in forcing terms while treating Y , β , and forcing terms as being mutually uncorrelated. In this paper we employ a two-dimensional finite element algorithm that is second-order accurate in σ_Y and zero-order accurate in σ_{β} and forcing terms. As the similar recursive approximations have been developed earlier by *Tartakovsky et al.* [2000], we do not discuss but merely summarize them here for completeness.

4.1. Recursive Conditional Mean Approximations

[18] Recursive equations for $\langle \Phi(\mathbf{x}) \rangle$ are given to zero order in σ_Y by

$$\nabla \cdot \left[K_G(\mathbf{x}) \left(\nabla \langle \Phi^{(0)}(\mathbf{x}) \rangle + g \alpha_G \langle \Phi^{(0)}(\mathbf{x}) \rangle \mathbf{e}_3 \right) \right] + \langle f(\mathbf{x}) \rangle = 0 \quad \mathbf{x} \text{ in } \Omega \quad (29)$$

$$\langle \Phi^{(0)}(\mathbf{x}) \rangle = \frac{1}{\alpha_G} e^{\alpha_G \Psi(\mathbf{x})} \quad \mathbf{x} \text{ on } \Gamma_D \quad (30)$$

$$\mathbf{n}(\mathbf{x}) \cdot \left[K_G(\mathbf{x}) \left(\nabla \langle \Phi^{(0)}(\mathbf{x}) \rangle + g \alpha_G \langle \Phi^{(0)}(\mathbf{x}) \rangle \mathbf{e}_3 \right) \right] = \langle Q(\mathbf{x}) \rangle \quad \mathbf{x} \text{ on } \Gamma_N \quad (31)$$

and to second order by

$$\begin{aligned}
\nabla \cdot \left[K_G(\mathbf{x}) \left(\nabla \langle \Phi^{(2)}(\mathbf{x}) \rangle + 0.5 \sigma_Y^2(\mathbf{x}) \nabla \langle \Phi^{(2)}(\mathbf{x}) \rangle \right) \right] - \mathbf{r}^{(2)}(\mathbf{x}) \\
+ g \alpha_G \left(K_G(\mathbf{x}) \left(\langle \Phi^{(2)}(\mathbf{x}) \rangle + 0.5 \sigma_Y^2(\mathbf{x}) \nabla \langle \Phi^{(0)}(\mathbf{x}) \rangle \right) \right) \\
+ R_{K\Phi}^{(2)}(\mathbf{x}) \mathbf{e}_3 \Big] = 0 \quad \mathbf{x} \text{ in } \Omega \quad (32)
\end{aligned}$$

$$\langle \Phi^{(2)}(\mathbf{x}) \rangle = 0 \quad \mathbf{x} \text{ on } \Gamma_D \quad (33)$$

$$\begin{aligned}
\mathbf{n}(\mathbf{x}) \cdot \left[K_G(\mathbf{x}) \left(\nabla \langle \Phi^{(2)}(\mathbf{x}) \rangle + 0.5 \sigma_Y^2(\mathbf{x}) \nabla \langle \Phi^{(2)}(\mathbf{x}) \rangle \right) \right] - \mathbf{r}^{(2)}(\mathbf{x}) \\
+ g \alpha_G \left(K_G(\mathbf{x}) \left(\langle \Phi^{(2)}(\mathbf{x}) \rangle + 0.5 \sigma_Y^2(\mathbf{x}) \nabla \langle \Phi^{(0)}(\mathbf{x}) \rangle \right) \right) \\
+ R_{K\Phi}^{(2)}(\mathbf{x}) \mathbf{e}_3 \Big] = 0 \quad \mathbf{x} \text{ on } \Gamma_N, \quad (34)
\end{aligned}$$

where the superscript () designates order of approximation in σ_Y , $K_G(\mathbf{x}) = \exp(\langle Y(\mathbf{x}) \rangle)$ is the conditional geometric mean of $Y(\mathbf{x})$, $\alpha_G = \exp(\langle \beta \rangle)$ is the geometric mean of α , $\sigma_Y^2(\mathbf{x}) = \langle Y'^2(\mathbf{x}) \rangle$ is the conditional variance of $Y(\mathbf{x})$, and

$$\begin{aligned}
\mathbf{r}^{(2)}(\mathbf{x}) = K_G(\mathbf{x}) \int_{\Omega} C_Y(\mathbf{x}, \mathbf{z}) \nabla_{\mathbf{x}} \nabla_{\mathbf{z}}^T \langle G^{(0)}(\mathbf{z}, \mathbf{x}) \rangle K_G(\mathbf{z}) \\
\cdot \left[\nabla \langle \Phi^{(0)}(\mathbf{z}) \rangle + g \alpha_G \langle \Phi^{(0)}(\mathbf{z}) \rangle \mathbf{e}_3 \right] d\Omega \quad (35)
\end{aligned}$$

$$\begin{aligned}
R_{K\Phi}^{(2)}(\mathbf{x}) = -K_G(\mathbf{x}) \int_{\Omega} C_Y(\mathbf{x}, \mathbf{z}) \nabla_{\mathbf{z}}^T \langle G^{(0)}(\mathbf{z}, \mathbf{x}) \rangle K_G(\mathbf{z}) \\
\cdot \left[\nabla \langle \Phi^{(0)}(\mathbf{z}) \rangle + g \alpha_G \langle \Phi^{(0)}(\mathbf{z}) \rangle \mathbf{e}_3 \right] d\Omega. \quad (36)
\end{aligned}$$

[19] The first-order approximation $\langle \Phi^{(1)}(\mathbf{x}) \rangle \equiv 0$ because it is governed by homogeneous equations. Recursive equations for the conditional mean flux $\langle \mathbf{q}(\mathbf{x}) \rangle$ are given to zero order in σ_Y by

$$\langle \mathbf{q}^{(0)}(\mathbf{x}) \rangle = -K_G(\mathbf{x}) \left(\nabla \langle \Phi^{(0)}(\mathbf{x}) \rangle + g \alpha_G \langle \Phi^{(0)}(\mathbf{x}) \rangle \mathbf{e}_3 \right) \quad (37)$$

and to second order by

$$\begin{aligned}
\langle \mathbf{q}^{(2)}(\mathbf{x}) \rangle = -K_G(\mathbf{x}) \left[\nabla \langle \Phi^{(2)}(\mathbf{x}) \rangle + \frac{\sigma_Y^2(\mathbf{x})}{2} \nabla \langle \Phi^{(0)}(\mathbf{x}) \rangle + g \alpha_G \right. \\
\cdot \left(\langle \Phi^{(2)}(\mathbf{x}) \rangle + \frac{\sigma_Y^2(\mathbf{x})}{2} \langle \Phi^{(0)}(\mathbf{x}) \rangle \right) \mathbf{e}_3 \Big] + \mathbf{r}^{(2)}(\mathbf{x}) \\
- g \alpha_G R_{K\Phi}^{(2)}(\mathbf{x}) \mathbf{e}_3. \quad (38)
\end{aligned}$$

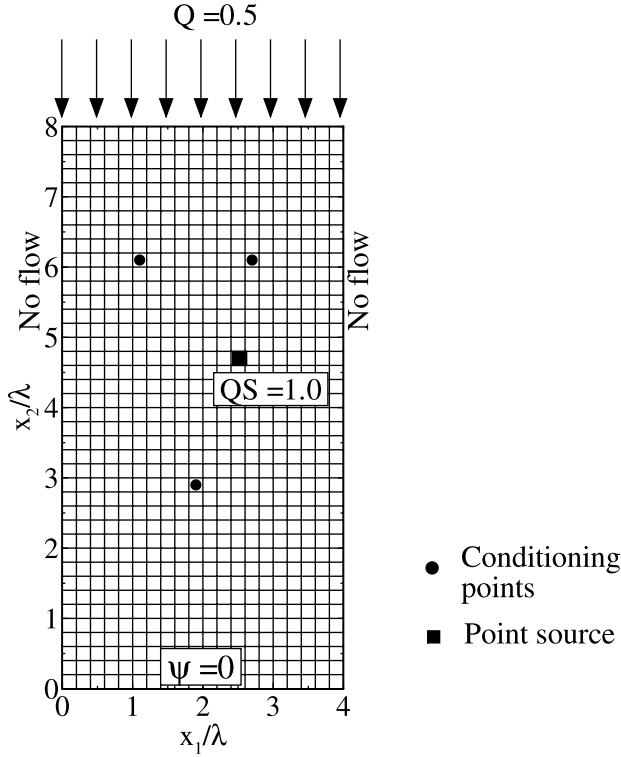


Figure 1. Definition of example problem, controlling parameters, and associated grid.

As the first-order term is zero, the total flux containing all terms to second order is

$$\mathbf{q}^{[2]}(\mathbf{x}) = \mathbf{q}^{(0)}(\mathbf{x}) + \mathbf{q}^{(2)}(\mathbf{x}). \quad (39)$$

4.2. Recursive Conditional Second Moment Approximations

[20] To second order in σ_Y the covariance function C_Φ is governed by

$$\nabla_x \cdot \mathbf{F}(\mathbf{x}, \mathbf{y}) = 0 \quad \mathbf{x} \text{ in } \Omega, \mathbf{y} \text{ in } \Omega \quad (40)$$

$$C_\Phi^{(2)}(\mathbf{x}, \mathbf{y}) = 0 \quad \mathbf{x} \text{ on } \Gamma_D, \mathbf{y} \text{ in } \Omega \quad (41)$$

$$\mathbf{n}(\mathbf{x}) \cdot \mathbf{F}(\mathbf{x}, \mathbf{y}) = 0 \quad \mathbf{x} \text{ on } \Gamma_N, \mathbf{y} \text{ in } \Omega, \quad (42)$$

where

$$\begin{aligned} \mathbf{F}(\mathbf{x}, \mathbf{y}) &= K_G(\mathbf{x}) \nabla_x C_\Phi^{(2)}(\mathbf{x}, \mathbf{y}) + C_{K\Phi}^{(2)}(\mathbf{x}, \mathbf{y}) \nabla \langle \Phi^{(0)}(\mathbf{x}) \rangle \\ &+ g \alpha_G \left(K_G(\mathbf{x}) C_\Phi^{(2)}(\mathbf{x}, \mathbf{y}) + C_{K\Phi}^{(2)}(\mathbf{x}, \mathbf{y}) \langle \Phi^{(0)}(\mathbf{x}) \rangle \right) \mathbf{e}_3 \end{aligned} \quad (43)$$

and $C_{K\Phi}^{(2)}(\mathbf{x}, \mathbf{y})$ is given by equations (B3) and (B4) in Appendix B.

[21] Recursive approximations for the conditional covariance tensor of flux, $\mathbf{C}_{\mathbf{q}\mathbf{q}}(\mathbf{x}, \mathbf{y}) = \langle \mathbf{q}'(\mathbf{x}) \mathbf{q}'^T(\mathbf{y}) \rangle$, are obtained upon multiplying equation (A10) by $\mathbf{q}'^T(\mathbf{y})$, taking ensemble mean, and expanding in powers of σ_Y and σ_β . To second order in σ_Y and zero order in σ_β this leads to

$$\begin{aligned} C_{\mathbf{q}\mathbf{q}}^{(2)}(\mathbf{x}, \mathbf{y}) &= K_G(\mathbf{x}) \left[\nabla_x \nabla_y^T C_\Phi^{(2)}(\mathbf{x}, \mathbf{y}) + \nabla_x C_{Y\Phi}^{(2)}(\mathbf{y}, \mathbf{x}) \right. \\ &\quad \cdot \nabla_y^T \langle \Phi^{(0)}(\mathbf{y}) \rangle + \nabla_y C_{Y\Phi}^{(2)}(\mathbf{x}, \mathbf{y}) \nabla_x^T \langle \Phi^{(0)}(\mathbf{x}) \rangle \\ &\quad \left. + C_Y(\mathbf{x}, \mathbf{y}) \nabla_x \langle \Phi^{(0)}(\mathbf{x}) \rangle \nabla_y^T \langle \Phi^{(0)}(\mathbf{y}) \rangle \right] K_G(\mathbf{y}) \\ &+ g \alpha_G K_G(\mathbf{x}) \left[\nabla_x C_\Phi^{(2)}(\mathbf{x}, \mathbf{y}) + \nabla_x C_{Y\Phi}^{(2)}(\mathbf{y}, \mathbf{x}) \right. \\ &\quad \cdot \langle \Phi^{(0)}(\mathbf{y}) \rangle + C_{Y\Phi}^{(2)}(\mathbf{x}, \mathbf{y}) \nabla_x \langle \Phi^{(0)}(\mathbf{x}) \rangle \\ &\quad \left. + C_Y(\mathbf{x}, \mathbf{y}) \nabla_x \langle \Phi^{(0)}(\mathbf{x}) \rangle \langle \Phi^{(0)}(\mathbf{y}) \rangle \right] \mathbf{e}_3^T K_G(\mathbf{y}) \\ &+ g \alpha_G \mathbf{e}_3 K_G(\mathbf{x}) \left[\nabla_y^T C_\Phi^{(2)}(\mathbf{x}, \mathbf{y}) + C_{Y\Phi}^{(2)}(\mathbf{y}, \mathbf{x}) \right. \\ &\quad \cdot \nabla_y^T \langle \Phi^{(0)}(\mathbf{y}) \rangle + \nabla_y^T C_{Y\Phi}^{(2)}(\mathbf{x}, \mathbf{y}) \langle \Phi^{(0)}(\mathbf{x}) \rangle + C_Y(\mathbf{x}, \mathbf{y}) \\ &\quad \cdot \langle \Phi^{(0)}(\mathbf{x}) \rangle \nabla_y^T \langle \Phi^{(0)}(\mathbf{y}) \rangle \left. \right] K_G(\mathbf{y}) + g \alpha_G^2 K_G(\mathbf{x}) \\ &\quad \cdot \left[C_\Phi^{(2)}(\mathbf{x}, \mathbf{y}) + C_{Y\Phi}^{(2)}(\mathbf{y}, \mathbf{x}) \langle \Phi^{(0)}(\mathbf{y}) \rangle + C_{Y\Phi}^{(2)}(\mathbf{x}, \mathbf{y}) \right. \\ &\quad \cdot \langle \Phi^{(0)}(\mathbf{x}) \rangle + C_Y(\mathbf{x}, \mathbf{y}) \langle \Phi^{(0)}(\mathbf{x}) \rangle \langle \Phi^{(0)}(\mathbf{y}) \rangle \left. \right] \mathbf{E}_3 K_G(\mathbf{y}), \end{aligned} \quad (44)$$

where

$$\begin{aligned} C_{Y\Phi}^{(2)}(\mathbf{x}, \mathbf{y}) &= - \int_{\Omega} C_Y(\mathbf{x}, \mathbf{y}) \nabla_z^T \langle G^{(0)}(\mathbf{z}, \mathbf{y}) \rangle K_G(\mathbf{z}) \\ &\quad \cdot \left[\nabla \langle \Phi^{(0)}(\mathbf{z}) \rangle + g \alpha_G \langle \Phi^{(0)}(\mathbf{z}) \rangle \mathbf{e}_3 \right] d\Omega, \end{aligned} \quad (45)$$

$G^{(0)}$ being a zero-order solution of equations (A5), (A6), and (A7) and \mathbf{E}_3 being a 3×3 null matrix with a single component equal to 1 at the intersection of the third row and third column.

4.3. Recursive Approximations for Conditional Moments of Pressure Head

[22] Once the boundary value problems equations (29), (30), and (31); (32), (33), and (34); and (40), (41), and (42) have been solved, one can continue by developing second-order approximations for the mean conditional pressure head, $\langle \psi^{[2]}(\mathbf{x}) \rangle = \langle \psi^{(0)}(\mathbf{x}) \rangle + \langle \psi^{(2)}(\mathbf{x}) \rangle$, and covariance, $C_\psi^{(2)}(\mathbf{x}, \mathbf{y})$. It follows from Appendix C that

$$\langle \psi^{(0)}(\mathbf{x}) \rangle = \frac{1}{\alpha_G} \ln \left[\alpha_G \langle \Phi^{(0)}(\mathbf{x}) \rangle \right] \quad (46)$$

$$\langle \psi^{(2)}(\mathbf{x}) \rangle = \frac{1}{\alpha_G} \left[\frac{\langle \Phi^{(2)}(\mathbf{x}) \rangle}{\langle \Phi^{(0)}(\mathbf{x}) \rangle} - \frac{1}{2} \frac{C_\Phi^{(2)}(\mathbf{x}, \mathbf{x})}{\langle \Phi^{(0)}(\mathbf{x}) \rangle^2} \right] \quad (47)$$

$$C_\psi^{(2)}(\mathbf{x}, \mathbf{y}) = \frac{1}{\alpha_G^2} \frac{C_\Phi^{(2)}(\mathbf{x}, \mathbf{y})}{\langle \Phi^{(0)}(\mathbf{x}) \rangle \langle \Phi^{(0)}(\mathbf{y}) \rangle}. \quad (48)$$

5. Numerical Implementation

[23] We solve the above recursive conditional moment equations by a Galerkin finite element scheme on a rectangular vertical grid with square elements, using bilinear weight functions. Our numerical scheme is similar in principle to that developed for

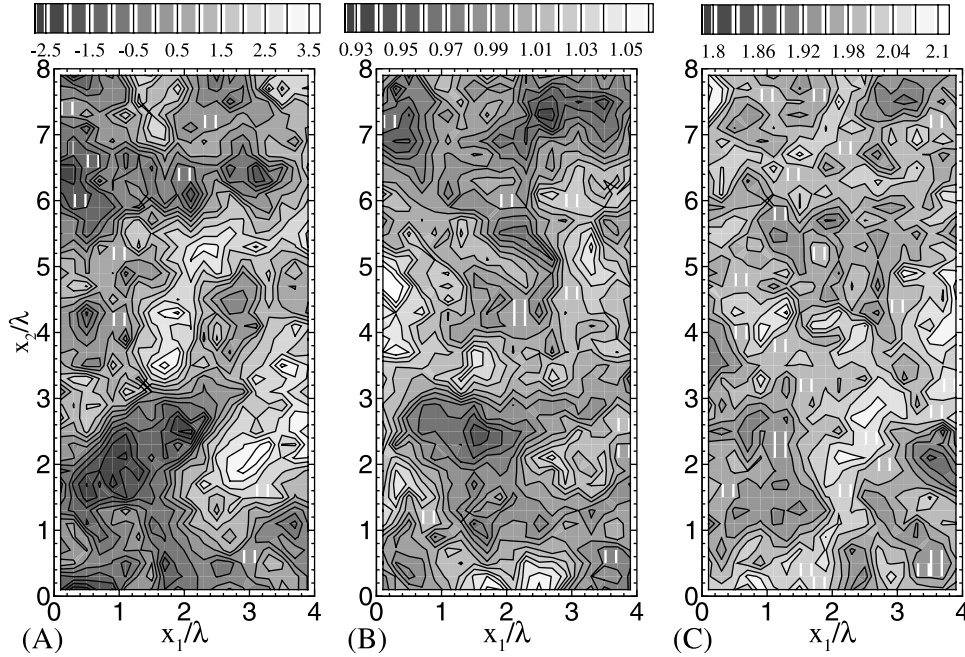


Figure 2. Images of (a) a single unconditional realization of $Y(\mathbf{x})$, (b) unconditional sample mean $\langle Y(\mathbf{x}) \rangle$, and (c) variance $\sigma_Y^2(\mathbf{x})$ based on 3000 Monte Carlo realizations with $\langle Y \rangle = 1$, $\sigma_Y^2 = 2$, and $\lambda = 1$.

saturated flow in a two-dimensional domain by *Guadagnini and Neuman* [1999b]. Details of our algorithm corresponding to these and higher-order recursive approximations are given by *Lu* [2000].

[24] To illustrate our computational approach, we consider a statistically homogeneous and isotropic log conductivity field Y with exponential autocovariance

$$C_Y(s) = \sigma_Y^2 e^{-s/\lambda}, \quad (49)$$

where s is separation distance, σ_Y^2 is the variance of Y , and λ is its autocorrelation scale. We adopt a rectangular grid of 20×40 square elements in the vertical plane (Figure 1) having width $L_1 = 4\lambda$, height $L_2 = 8\lambda$, and elements with sides 0.2λ . Boundary conditions consist of no flow on the left and right sides ($x_1 = 0$ and $x_1 = 4.0\lambda$), a constant deterministic flux $Q = 0.5$ (all terms are given in arbitrary consistent units) at the top boundary ($x_2 = 8.0\lambda$), and zero-pressure head at the bottom ($x_2 = 0$). A point source of magnitude $QS = 1$ is

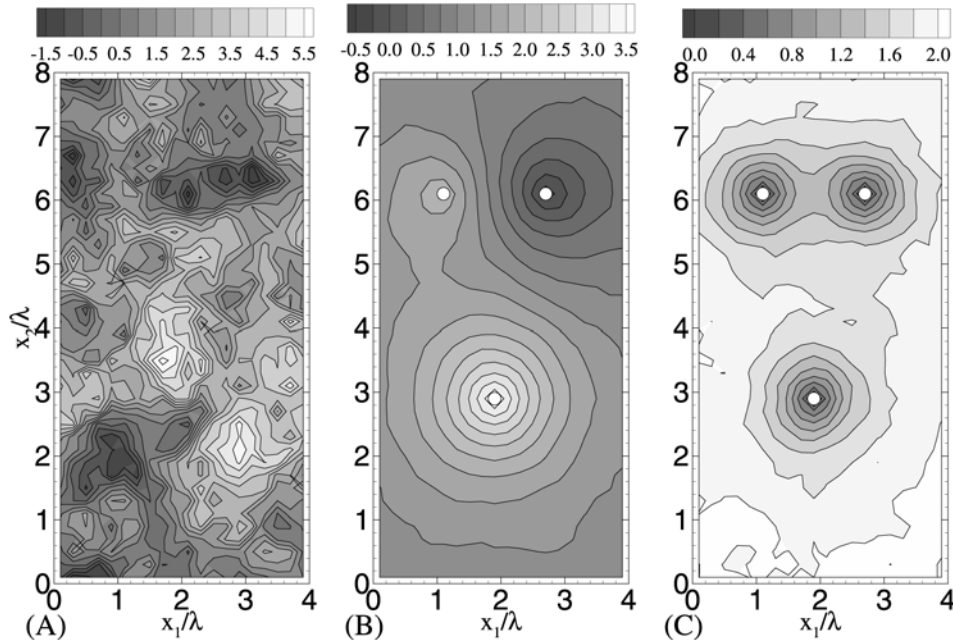


Figure 3. Images of (a) a single conditional realization of $Y(\mathbf{x})$, (b) conditional sample mean $\langle Y(\mathbf{x}) \rangle$, and (c) variance $\sigma_Y^2(\mathbf{x})$ based on 3000 Monte Carlo realizations with $\langle Y \rangle = 1$, $\sigma_Y^2 = 2$, and $\lambda = 1$.

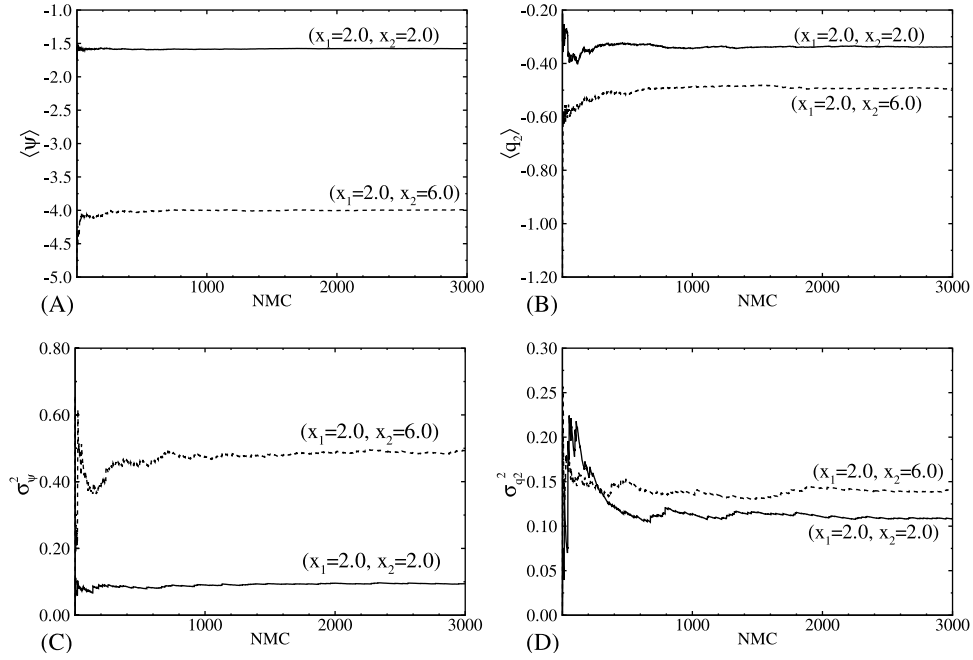


Figure 4. Variation of conditional (a) mean pressure head, (b) mean longitudinal flux, (c) variance of pressure head, and (d) variance of longitudinal flux at two points with number of Monte Carlo (NMC) simulations for $\sigma_Y^2 = 2$.

placed inside the domain to render the flow locally divergent. The saturated hydraulic conductivity field is made statistically non-homogeneous through conditioning at three points, two above and one below the source.

[25] To solve the original stochastic flow equations by numerical Monte Carlo simulation, we took Y to be multivariate Gaussian (this is not required for our conditional moment solution, which is free of distributional assumptions). We started by generating 3000 unconditional random Y realizations on our grid using a Gaussian sequential simulator, GCOSIM [Gómez-Hernández, 1991], with $\langle Y \rangle = 1$, $\sigma_Y^2 = 2$, and $\lambda = 1$. For purposes of flow analysis by conditional Monte Carlo simulation we assigned to each element a

constant Y value corresponding to the point value generated at its center by GCOSIM. This is justified considering that our grid includes a minimum of five such cells per unit autocorrelation scale. Figure 2 shows images of a single unconditional realization, unconditional sample mean $\langle Y(\mathbf{x}) \rangle$, and variance $\sigma_Y^2(\mathbf{x})$ obtained from these simulations. The sample mean and variance are quite close to their theoretical counterparts, ranging from 0.93 to 1.07 and from 1.85 to 2.12, respectively. The unconditional autocovariance C_Y obtained from Monte Carlo simulations compares favorably with that given theoretically by equation (49).

[26] We selected one of the above unconditional realizations of Y and took its values at the conditioning points to represent exact

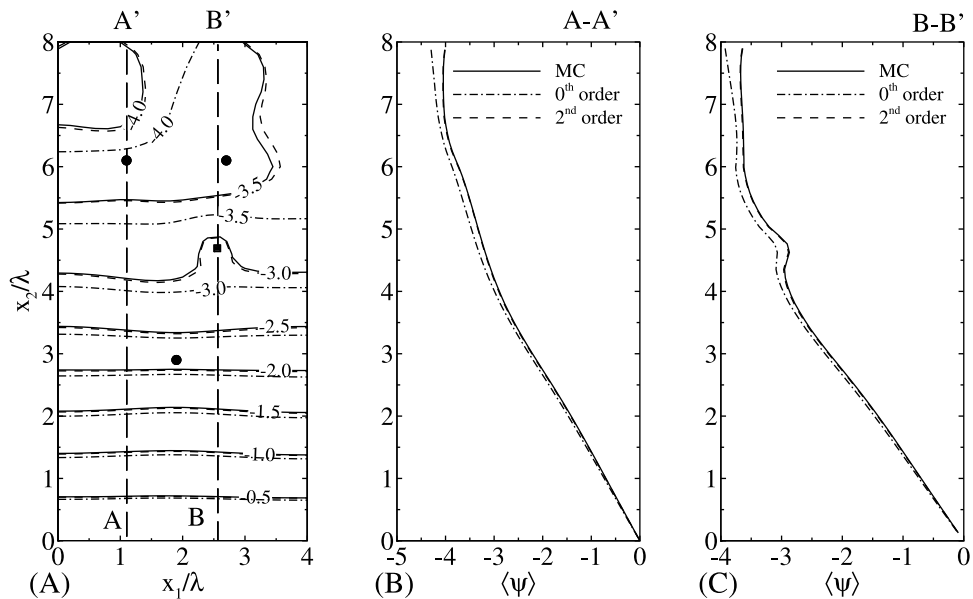


Figure 5. Contours and profiles of conditional mean pressure head obtained by Monte Carlo (MC) and zero- and second-order recursive solutions for $\sigma_Y^2 = 2$.

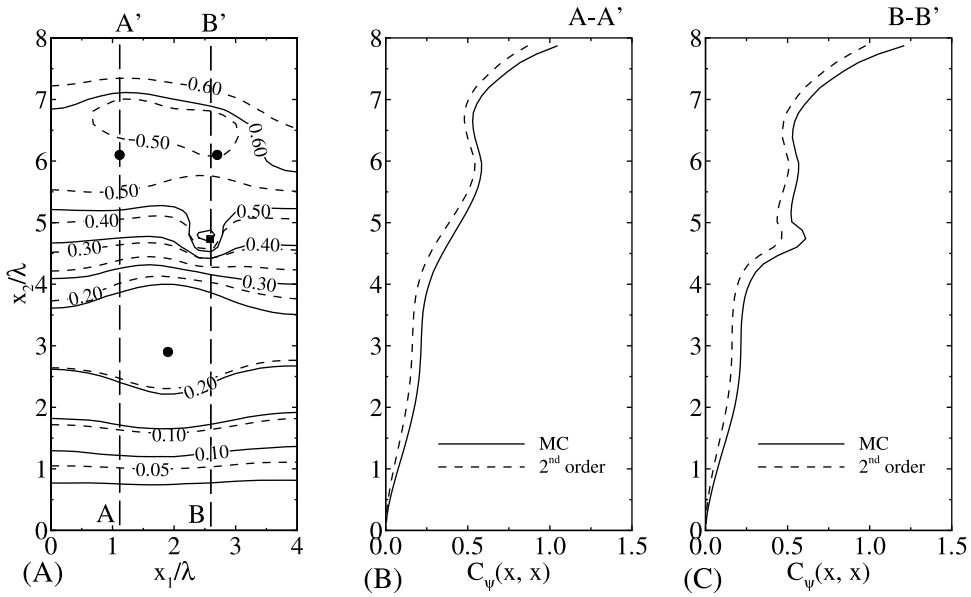


Figure 6. Contours and profiles of conditional variance of pressure head obtained by MC and second-order recursive solutions for $\sigma_Y^2 = 2$.

“measurements.” We then generated number of Monte Carlo simulations (NMC) = 3000 corresponding conditional realizations of Y by the same method. Figure 3 shows images of a single conditional realization, conditional sample mean $\langle Y(\mathbf{x}) \rangle$, and conditional variance $\sigma_Y^2(\mathbf{x})$ obtained from these simulations.

[27] We solved equations (1), (2), (3), and (4) for each unconditional and conditional realization of Y by standard finite elements using $\ln \alpha = -1$. We did so by using standard Galerkin finite elements with bilinear interpolation. Both the grid and the method of solution are fully compatible with the finite element methodology that we use to solve the corresponding nonlocal moment equations. To insure similar compatibility between conditional

moments in the Monte Carlo and nonlocal flow solutions, we employed in the latter conditional moments of $Y(\mathbf{x})$ that had been estimated from corresponding sample realizations (in practical applications one would normally infer these moments geostatistically from measurements by methods such as kriging). We then calculated corresponding sample mean pressure head and flux at each node as well as sample variance and covariance of pressure head and flux across the grid, based on all 3000 conditional Monte Carlo solutions of equations (1), (2), (3), and (4). This completed our conditional Monte Carlo simulation.

[28] All quantities which enter into our conditional moment equations are generally much smoother than their random (and

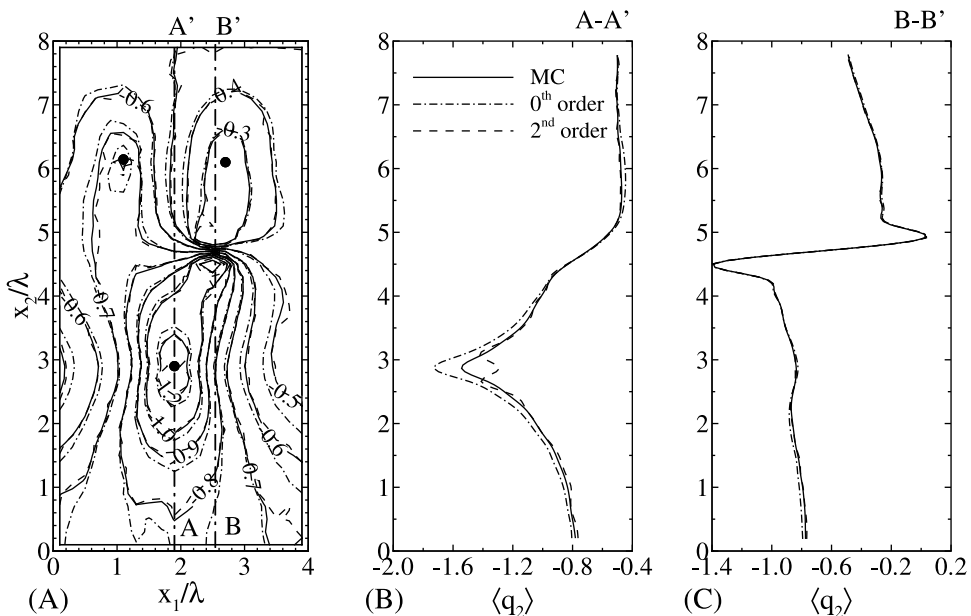


Figure 7. Contours and profiles of conditional mean longitudinal (vertical) flux obtained by MC and zero- and second-order recursive solutions for $\sigma_Y^2 = 2$.

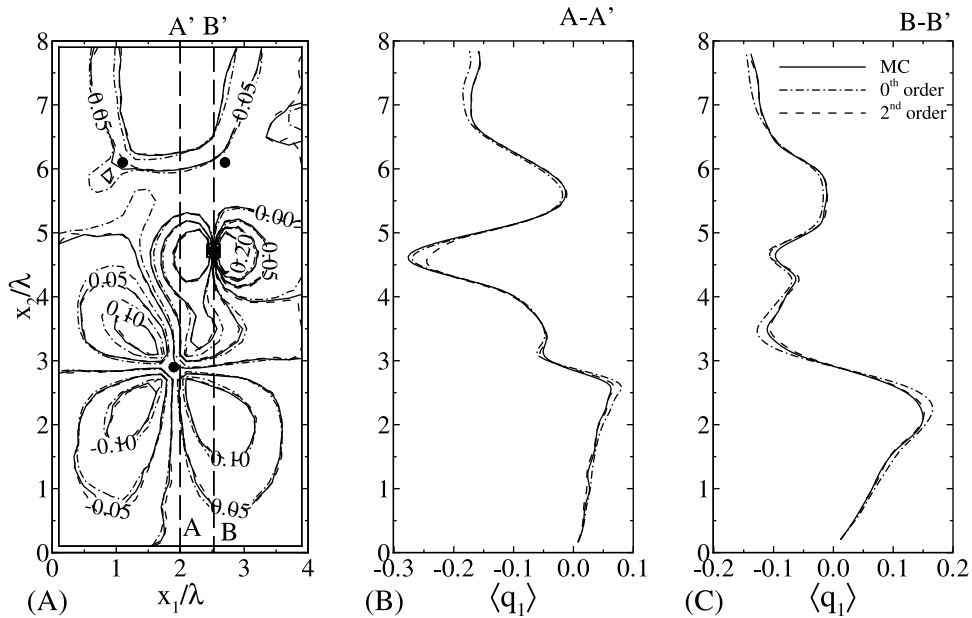


Figure 8. Contours and profiles of conditional mean transverse (horizontal) flux obtained by MC and zero- and second-order recursive solutions for $\sigma_y^2 = 2$.

therefore at best partially known) counterparts. This allows solving them numerically on a computational grid that is defined a posteriori, based on the degree of smoothness one expects the moment functions to exhibit, rather than a priori on the basis of more or less ad hoc criteria, as is common when one uses upscaling. The degree of smoothness exhibited by the moment functions is controlled, to a large extent, by the distribution of conditioning points in space. In most cases, such points are sparse enough to insure that the conditional mean functions fluctuate at lower spatial frequencies than do their random counterparts. Hence the grid required to resolve the former is generally coarser than that

required to resolve the latter. In this paper we nevertheless employ a fine grid to allow comparing our conditional mean flow results directly with numerical Monte Carlo solutions of the original stochastic Richards' equation.

6. Results and Discussions

[29] We focus on computational results obtained by the two methods and their comparative analysis. We start by examining the rate at which the Monte Carlo (MC) solution converges to a stable solution. We then compare Monte Carlo and zero- as well as

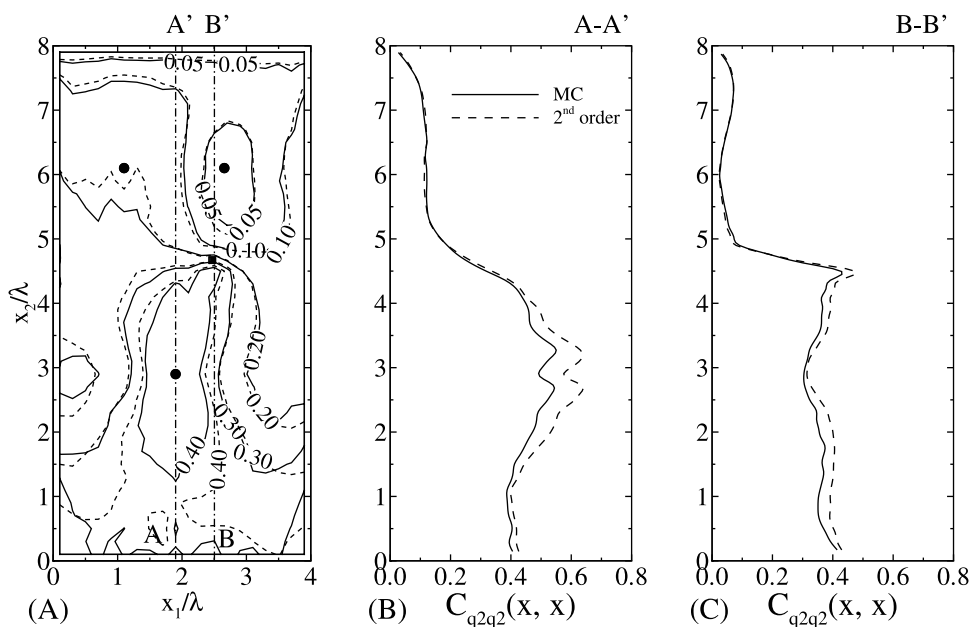


Figure 9. Contours and profiles of conditional variance of longitudinal flux obtained by MC and second-order recursive solutions for $\sigma_y^2 = 2$.

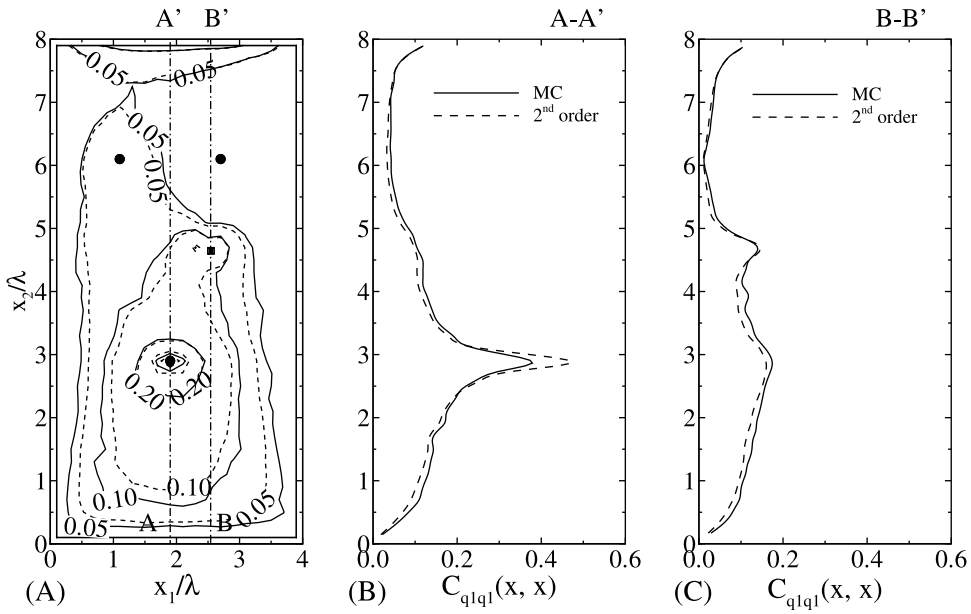


Figure 10. Contours and profiles of conditional variance of transverse flux obtained by MC and second-order recursive solutions for $\sigma_Y^2 = 2$.

second-order recursive finite element results for the conditional case, followed by a similar comparison for the unconditional case.

6.1. Conditional Simulations

[30] Figure 4 illustrates how conditional mean pressure head, conditional mean longitudinal (vertical) flux, conditional variance of mean pressure head, and conditional variance of longitudinal flux vary with the number NMC of Monte Carlo simulations at two points ($x_1 = 2, x_2 = 2$ and $x_1 = 2, x_2 = 6$) in the grid depicted in Figure 1. Whereas the conditional mean pressure head, conditional mean longitudinal flux, and conditional variance of pressure head require only of the order of NMC = 2000 to stabilize at these two

points, the conditional variance of longitudinal flux requires at least NMC = 3000. In this paper we do not require that the MC moments stabilize fully, only that they stabilize partially and be comparable to those we compute directly by our recursive finite element algorithm. We achieve this by working with a sample of NMC = 3000 realizations and adopting the corresponding sample statistics of Y , rather than its ensemble statistics, as input into our recursive finite element model.

6.1.1. Mean conditional pressure head. [31] Figure 5a compares conditional mean contours of pressure head ψ obtained by MC simulation (solid line) and zero-order (dash-dotted line) and second-order (dashed line) recursive finite element solutions on the

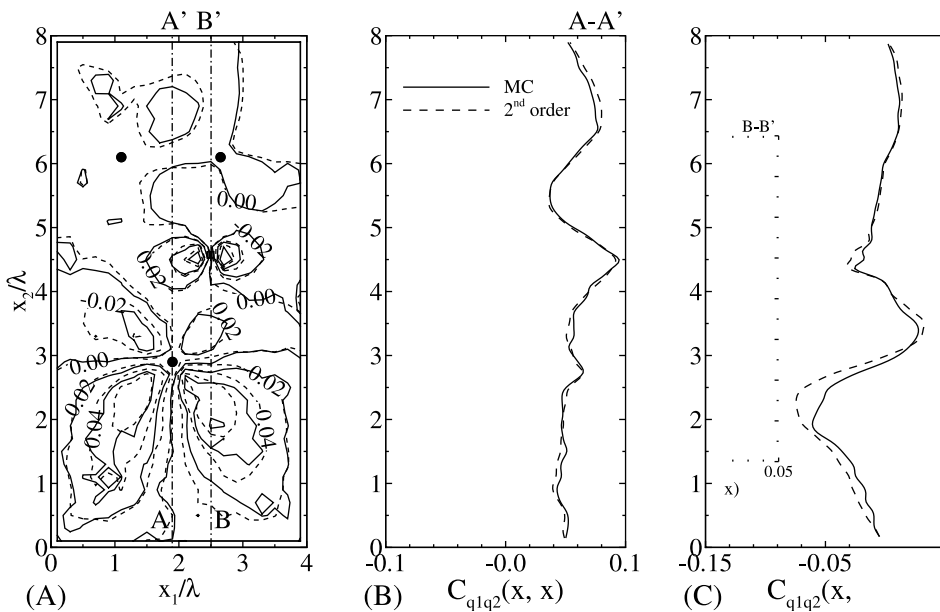


Figure 11. Contours and profiles of one-point conditional cross-covariance between transverse and longitudinal fluxes obtained by MC and second-order recursive solutions for $\sigma_Y^2 = 2$.

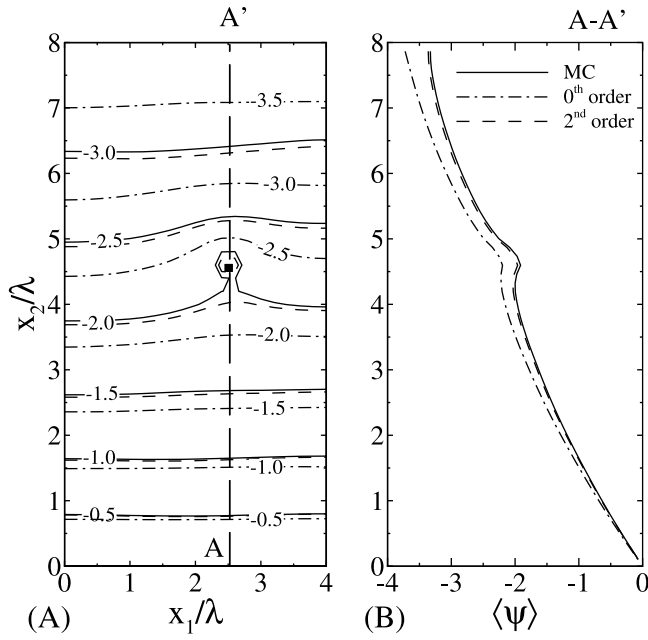


Figure 12. Contours and profiles of unconditional mean pressure head obtained by MC and zero- and second-order recursive solutions for $\sigma_Y^2 = 2$.

grid and under the conditions depicted in Figure 1. Figure 5b shows the same along a vertical profile passing through one of the conditioning points, and Figure 5c shows the same along a similar profile passing through the point source. The second-order mean pressure head virtually coincides with Monte Carlo results, with a maximum difference of 0.8% and average difference of 0.3% between the two sets of results across the grid. The zero-order solution deviates from the Monte Carlo results by as much as 10.5% near the upper prescribed flux boundary but only 3.2% on average across the grid.

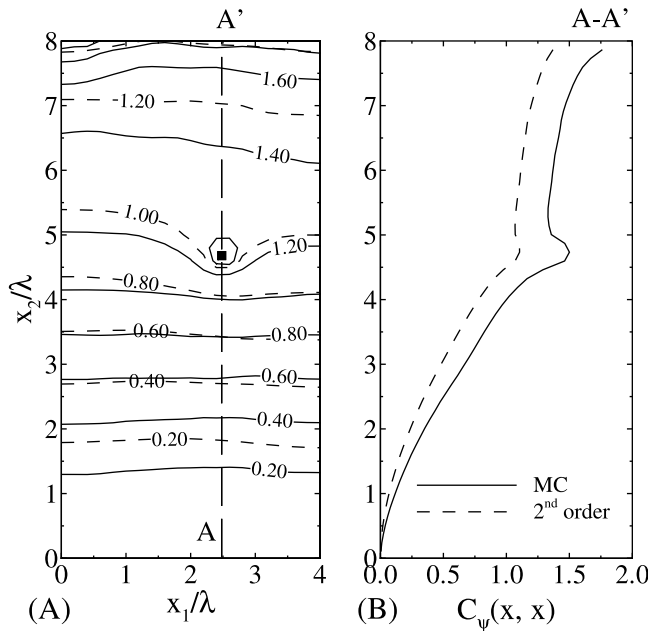


Figure 13. Contours and profiles of unconditional variance of pressure head obtained by MC and second-order recursive solutions for $\sigma_Y^2 = 2$.

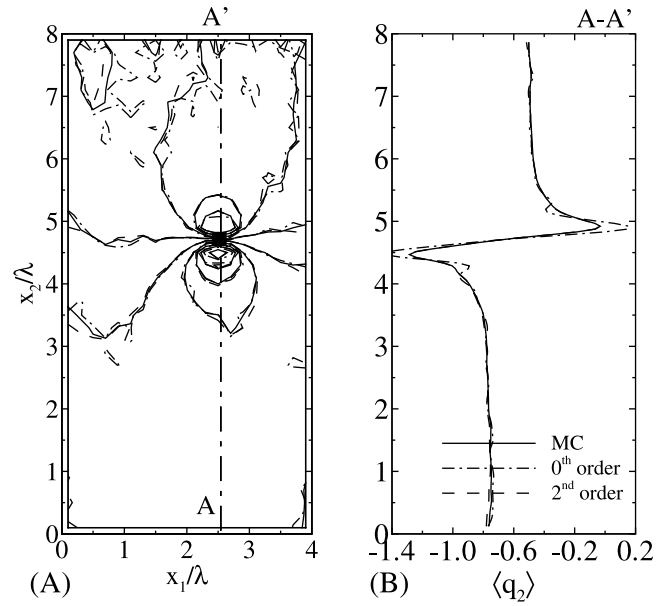


Figure 14. Contours and profiles of unconditional mean longitudinal (vertical) flux obtained by MC and zero- and second-order recursive solutions for $\sigma_Y^2 = 2$.

6.1.2. Conditional variance of pressure head. [32] Figure 6a compares contours of conditional pressure head variance as obtained by MC and second-order finite elements. Figures 6b and 6c show how this variance varies along profiles indicated on Figure 6a. Although our second-order results represent only the lowest possible order of approximating second moments, the corresponding variance of pressure head is close to the Monte Carlo results, even though the underlying Y field is quite strongly heterogeneous with unconditional variance as large as $\sigma_Y^2 = 2$. With the exception of a peak at the source (Figure 6c), the variance of ψ

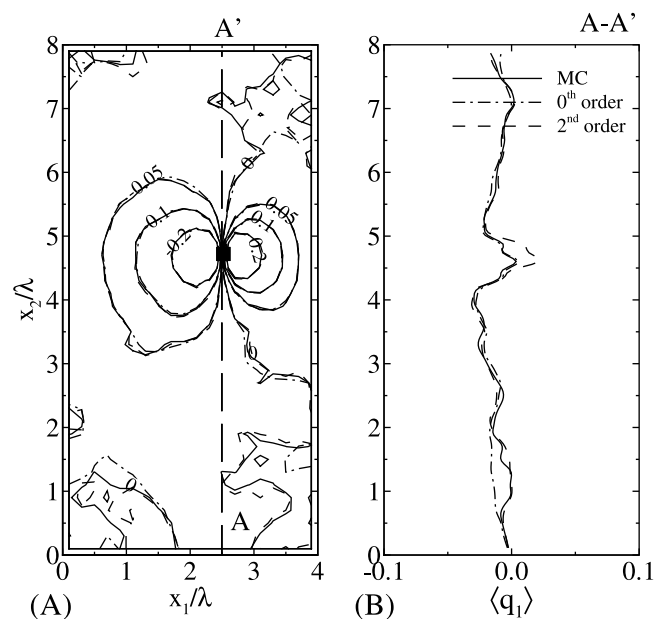


Figure 15. Contours and profiles of unconditional mean transverse (horizontal) flux obtained by MC and zero- and second-order recursive solutions for $\sigma_Y^2 = 2$.

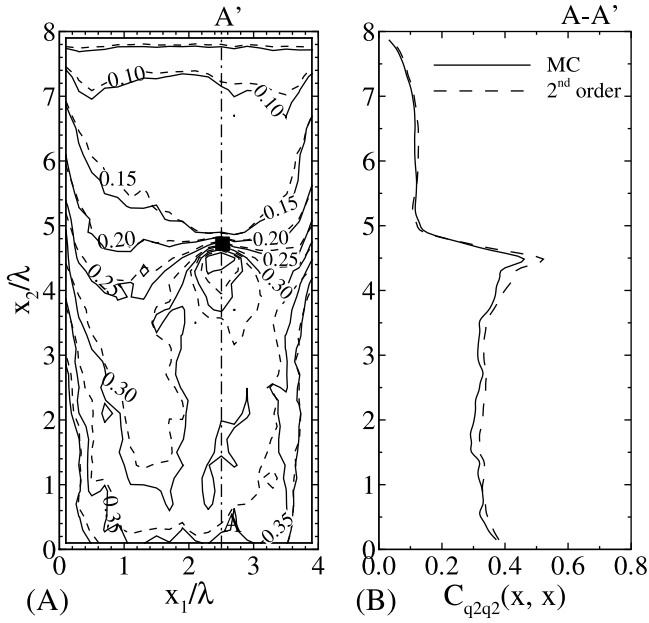


Figure 16. Contours and profiles of unconditional variance of longitudinal flux obtained by MC and second-order recursive solutions for $\sigma_Y^2 = 2$.

is zero at the bottom Dirichlet boundary and increases with vertical distance above this boundary.

6.1.3. Conditional mean flux. [33] Figure 7 compares conditional mean flux in the longitudinal (vertical) x_2 direction as obtained by Monte Carlo simulation and zero-order and second-order conditional moment solutions. Both the zero- and second-order solutions compare favorably with Monte Carlo results, the latter being slightly better than the former. The mean longitudinal

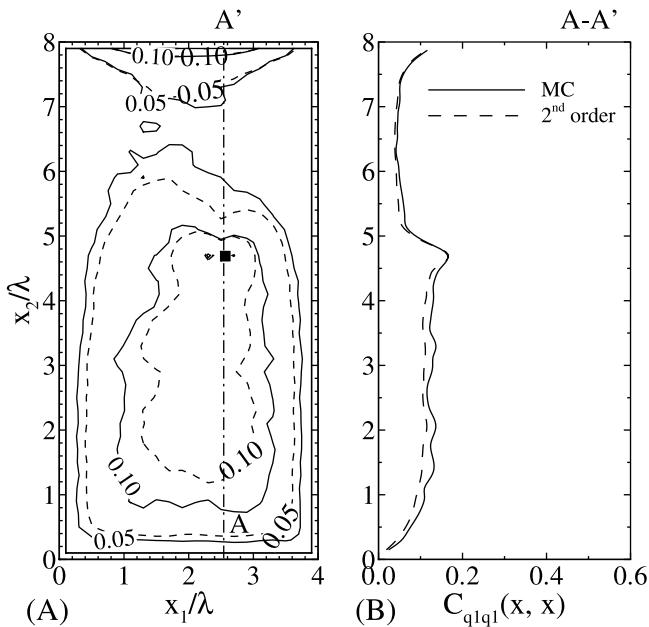


Figure 17. Contours and profiles of unconditional variance of transverse flux obtained by MC and second-order recursive solutions for $\sigma_Y^2 = 2$.

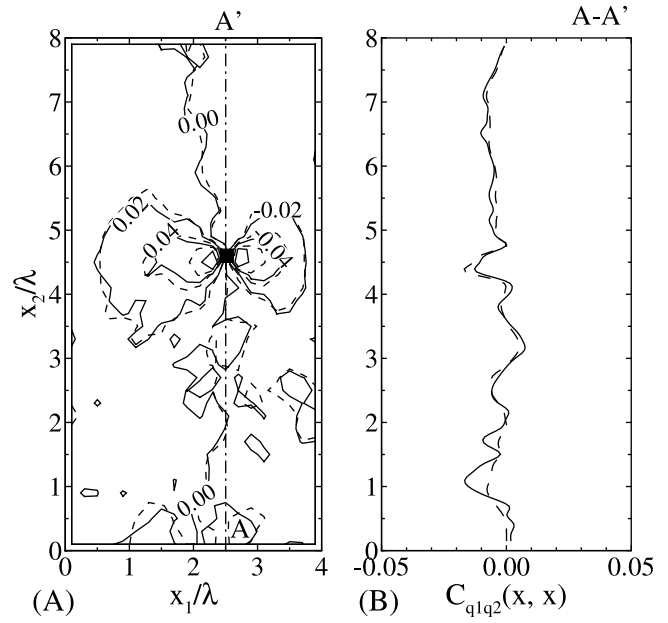


Figure 18. Contours and profiles of one-point unconditional cross-covariance between transverse and longitudinal fluxes obtained by MC and second-order recursive solutions for $\sigma_Y^2 = 2$.

flux field is strongly influenced by conditioning points and the point source, which render it distinctly nonuniform. To help explain the resulting longitudinal flux pattern, we refer the reader to a contour map of conditional mean log saturated conductivities $\langle Y \rangle$ in Figure 3b. This map shows that the upper right conditioning point corresponds to a local drop in $\langle Y \rangle$. Therefore the contours in Figure 7a show a reduction in the magnitude of mean longitudinal flux toward this point. At the other two conditioning points, $\langle Y \rangle$ exhibits a peak. Therefore the magnitude of mean longitudinal flux increases toward each of these two conditioning points. Near the point source, closely spaced contours of mean longitudinal flux reflect a very rapid change in its magnitude along the vertical.

[34] Figure 8 compares conditional mean flux in the transverse (horizontal) x_1 direction as obtained by Monte Carlo simulation and zero-order and second-order conditional moment solutions. Again, both the zero- and second-order solutions compare favorably with Monte Carlo results, the latter being slightly better than the former. The mean transverse flux field is strongly influenced by conditioning points and the point source, which render it markedly nonuniform. Owing to a pronounced peak in $\langle Y \rangle$ at the lower conditioning point, mean transverse flux converges toward it on the upstream side and away from it on the downstream side. Symmetry is broken by the point source, which causes the mean transverse flux to exhibit a steep horizontal gradient in its vicinity.

6.1.4. Conditional variance-covariance tensor of flux. [35] Figure 9 compares the conditional variance of longitudinal flux $C_{q_2 q_2}^{(2)}(x, x)$, as obtained by Monte Carlo simulation, and the second-order conditional moment approach. Figures 10 and 11 do the same for the conditional variance of transverse flux $C_{q_1 q_1}^{(2)}(x, x)$ and one-point cross-covariance between longitudinal and transverse flux $C_{q_1 q_2}^{(2)}(x, x) = C_{q_2 q_1}^{(2)}(x, x)$, respectively. There is excellent agreement between the two solutions in all three cases.

[36] As seen in Figure 9, the conditional variance of longitudinal flux generally increases from zero at the upper prescribed

flux boundary toward the bottom prescribed pressure head boundary. The conditional variance of transverse flux is zero at the bottom boundary and the vertical no-flow boundaries, increasing systematically toward the center of the domain (Figure 10). Both the longitudinal and transverse variances are relatively large at the lower and upper left conditioning points (at which $\langle Y \rangle$ is large) and the point source (at which mean longitudinal and transverse flux gradients are large). Both variances are relatively small at the upper right conditioning point (at which $\langle Y \rangle$ is small). The conditional cross-covariance between longitudinal and transverse fluxes does not show any systematic trend across the domain (Figure 11). The cross-covariance is zero at the point source and peaks at the lower conditioning point. Its spatial pattern is reminiscent of that exhibited in Figure 7 by the conditional mean transverse flux.

6.2. Unconditional Simulations

[37] We now examine briefly the effect of eliminating the conditioning points in the previous example. All other aspects of the problem remain the same as in the conditional case.

6.2.1. Mean unconditional pressure head. [38] Figure 12 compares unconditional mean pressure head ψ , obtained by Monte Carlo (MC) simulation, and zero- and second-order recursive finite element solutions on the grid and under the conditions depicted in Figure 1 but without the inclusion of conditioning points. Because of the absence of such points, the mean pressure head now varies more uniformly across the domain than it did in the conditional case depicted in Figure 5. The second-order mean pressure head is still very close to the Monte Carlo results but slightly less so than in the conditional case. Though contours of the zero-order unconditional mean pressure head deviate considerably from those representing Monte Carlo results, the two solutions are seen in longitudinal (vertical) profile to be quite close. The contour map exaggerates the difference between these two solutions because of the relatively flat outline of the profile.

6.2.2. Unconditional variance of pressure head. [39] Figure 13 compares the unconditional variance of pressure head as obtained by Monte Carlo and second-order finite elements. A comparison with Figure 6 shows that conditioning reduces the variance of pressure head and improves the quality of the second-order solution by bringing it closer to the Monte Carlo results.

6.2.3. Unconditional mean flux. [40] Figures 14 and 15 compare unconditional mean longitudinal and transverse fluxes, respectively, as obtained by Monte Carlo simulation and zero-order and second-order conditional moment solutions. Both the zero- and second-order solutions compare favorably with Monte Carlo results, the latter being slightly better than the former. Both the longitudinal and transverse flow patterns are vastly different from their conditional counterparts in Figures 7 and 8.

6.2.4. Unconditional variance-covariance tensor of flux. [41] Figures 16, 17, and 18 compare second-order and Monte Carlo solutions for the unconditional variance of longitudinal and transverse fluxes. Here the quality of the second-order solutions is as good as it was in the conditional case, depicted in Figures 9, 10, and 11. The patterns, however, are often quite different owing to the absence of conditioning points. A comparison of Figures 9 and 10 and Figures 16 and 17 reveals that conditioning may locally increase the variance of both longitudinal and transverse flux, as happens most evidently at the lower conditioning point (at which conditional mean log conductivity exhibits a pronounced peak). Upon comparing Figures 11 and 18, one notes that conditioning has brought about

an increase in the one-point cross-covariance between transverse and longitudinal fluxes.

7. Conclusions

[42] This paper leads to the following major conclusions.

1. It is possible to render optimum unbiased predictions of steady state unsaturated flow in bounded, randomly heterogeneous soils under the influence of uncertain boundary and source terms, deterministically without upscaling or linearizing the constitutive relation between hydraulic conductivity and pressure head. It is likewise possible to quantify the uncertainty of such predictions. The approach works when this relation is represented by *Gardner's* [1958] exponential model, in which the exponent α is a random constant and saturated hydraulic conductivity K_s is a spatially correlated random field. The approach is based on recursive approximations of exact integro-differential equations for the conditional mean and variance-covariance of Kirchhoff-transformed pressure head and flux.

2. The above recursive approximations are amenable to discretization by means of finite elements. We have done so for two-dimensional unsaturated flow to second order in the standard deviation of $Y = \ln K_s$ and zero order in the standard deviations of $\beta = \ln \alpha$ as well as forcing terms. Our algorithm is similar in principle to that developed for two-dimensional saturated flow by *Guadagnini and Neuman* [1999b].

3. Our computational results are nominally restricted to mildly heterogeneous media with $\sigma_Y^2 \ll 1$. Nevertheless, when we compare our moment solution for two-dimensional superimposed mean uniform and convergent flows with conditional and unconditional Monte Carlo finite element simulations, we find that the former is remarkably accurate (more so in the conditional than in the unconditional case) for strongly heterogeneous soils with σ_Y^2 as large as 2. This accords well with a theoretical analysis by *Tartakovsky et al.* [1999], which shows that the solution may remain asymptotic for σ_Y^2 values as large as 2. We have not tested the performance of our conditional moment algorithm for σ_Y^2 values larger than 2 but note that *Guadagnini and Neuman* [1999b] had obtained very good results with a similar algorithm under saturated flow for σ_Y^2 as large as 4. Whether the same would hold true in our unsaturated case is presently unclear.

4. Our recursive finite element algorithm shares with *Zhang and Winter* [1998], *Zhang et al.* [1998], and *Zhang* [1999] the reliance on conditional moment approximations for unsaturated flow. However, it differs from their approach by obviating the need to introduce perturbation approximations for the soil constitutive relations and has been shown by us to work well under the adverse conditions of a strongly heterogeneous soil with a point source. Another advantage of our approach is that once the auxiliary functions have been determined for a given set of conditioning points and boundary types, one can use them to solve a large number of related stochastic flow problems subject to different boundary terms and an unlimited range of source terms. Computing the auxiliary functions simultaneously on parallel processors could potentially enhance the computational efficiency of our algorithm.

5. Our computational results demonstrate that conditioning improves the quality of the recursive finite element solution and reduces the prediction variance of pressure head. Whereas conditioning may impact markedly the predicted flux pattern, it does not necessarily reduce the variance of predicted flux and may locally cause this variance to increase. The effect of a point source is to significantly alter the predicted flux pattern and increase the prediction variance of both pressure head and flux.

6. Although our second-order finite element results are superior to zero-order results in all cases, the zero-order approximations of flux tend to be highly accurate in both the conditional and unconditional cases. However, second-order approximations are always required for the assessment of uncertainty in predicted pressure head and flux.

Appendix A

[43] Substituting equations (12), (13), and (14) into equations (8), (9), and (10) and subtracting the corresponding conditional mean equations (15), (16), and (17) yield the following implicit equations for $\Phi'(\mathbf{x})$:

$$\nabla \cdot F(\mathbf{x}) + f'(\mathbf{x}) = 0 \quad \mathbf{x} \text{ in } \Omega \quad (\text{A1})$$

$$\Phi'(\mathbf{x}) = H'(\mathbf{x}) \quad \mathbf{x} \text{ on } \Gamma_D \quad (\text{A2})$$

$$\mathbf{n}(\mathbf{x}) \cdot F(\mathbf{x}) = Q'(\mathbf{x}) \quad \mathbf{x} \text{ on } \Gamma_N \quad (\text{A3})$$

$$\begin{aligned} F(\mathbf{x}) &= K_s(\mathbf{x})\nabla\Phi'(\mathbf{x}) + K'_s(\mathbf{x})\nabla\langle\Phi(\mathbf{x})\rangle + \mathbf{r}(\mathbf{x}) \\ &+ g(\alpha K_s(\mathbf{x})\Phi'(\mathbf{x}) + \alpha'K'_s(\mathbf{x})\langle\Phi(\mathbf{x})\rangle + \langle\alpha\rangle K'_s(\mathbf{x})\langle\Phi(\mathbf{x})\rangle \\ &- \langle\alpha\rangle R_{K\Phi}(\mathbf{x}) - \langle K_s(\mathbf{x})\rangle R_{\alpha\Phi}(\mathbf{x}) - R_{\alpha K\Phi}(\mathbf{x}))\mathbf{e}_3. \end{aligned} \quad (\text{A4})$$

[44] To obtain an explicit expression for $\Phi'(\mathbf{x})$, we introduce an auxiliary random function $G(\mathbf{y}, \mathbf{x})$ that satisfies

$$\begin{aligned} \nabla_{\mathbf{y}} \cdot [K_s(\mathbf{y})\nabla_{\mathbf{y}}G(\mathbf{y}, \mathbf{x})] - g\alpha\mathbf{e}_3^T K_s(\mathbf{y})\nabla_{\mathbf{y}}G(\mathbf{y}, \mathbf{x}) \\ + \delta(\mathbf{x} - \mathbf{y}) = 0 \quad \mathbf{y} \text{ in } \Omega, \mathbf{x} \text{ in } \Omega \end{aligned} \quad (\text{A5})$$

$$G(\mathbf{y}, \mathbf{x}) = 0 \quad \mathbf{y} \text{ on } \Gamma_D, \mathbf{x} \text{ in } \Omega \quad (\text{A6})$$

$$\nabla_{\mathbf{y}}G(\mathbf{y}, \mathbf{x}) \cdot \mathbf{n}(\mathbf{y}) = 0 \quad \mathbf{y} \text{ on } \Gamma_N, \mathbf{x} \text{ in } \Omega, \quad (\text{A7})$$

where δ is the Dirac delta. Unlike the symmetric Green's function presented by *Guadagnini and Neuman* [1999a] for saturated flow, here G is nonsymmetric. Rewriting equations (A1), (A2), (A3), and (A4) in terms of \mathbf{y} , multiplying by G , integrating with respect to \mathbf{y} over Ω , and applying Green's first identity yields the desired expression

$$\begin{aligned} \Phi'(\mathbf{x}) &= - \int_{\Omega} \nabla_{\mathbf{y}}^T G(\mathbf{y}, \mathbf{x}) [K'_s(\mathbf{y})\nabla\langle\Phi(\mathbf{y})\rangle + \mathbf{r}(\mathbf{y}) \\ &+ g(\alpha'K_s(\mathbf{y})\langle\Phi(\mathbf{y})\rangle + \langle\alpha\rangle K'_s(\mathbf{y})\langle\Phi(\mathbf{y})\rangle - \langle\alpha\rangle R_{K\Phi}(\mathbf{y}) \\ &- \langle K_s(\mathbf{y})\rangle R_{K\Phi}(\mathbf{y}) - R_{\alpha K\Phi}(\mathbf{y}))\mathbf{e}_3] d\Omega + \int_{\Omega} f'(\mathbf{y})G(\mathbf{y}, \mathbf{x})d\Omega \\ &+ \int_{\Gamma_N} G(\mathbf{y}, \mathbf{x})Q'(\mathbf{y})d\Gamma - \int_{\Gamma_D} H'(\mathbf{y})K_s(\mathbf{y})\nabla_{\mathbf{y}}G(\mathbf{y}, \mathbf{x}) \cdot \mathbf{n}(\mathbf{y})d\Gamma. \end{aligned} \quad (\text{A8})$$

[45] Introducing equations (6) and (7) into equation (1) gives

$$\mathbf{q}(\mathbf{x}) = -K_s(\mathbf{x})[\nabla\Phi(\mathbf{x}) + g\alpha\Phi(\mathbf{x})\mathbf{e}_3]. \quad (\text{A9})$$

Writing $\mathbf{q}(\mathbf{x}) = \langle\mathbf{q}(\mathbf{x})\rangle + \mathbf{q}'(\mathbf{x})$, substituting equations (12), (13), and (14) into (A9) and taking conditional ensemble mean leads to

equation (18). Subtracting equation (18) from equation (A9) and using equations (12), (13), and (14) yields

$$\begin{aligned} \mathbf{q}'(\mathbf{x}) &= -\langle K_s(\mathbf{x})\rangle \left(\nabla\Phi'(\mathbf{x}) + g(\langle\alpha\rangle\Phi'(\mathbf{x}) + \alpha'\Phi(\mathbf{x}))\mathbf{e}_3 \right) \\ &- K'_s(\mathbf{x})(\nabla\Phi(\mathbf{x}) + g\alpha\Phi(\mathbf{x})\mathbf{e}_3) - \mathbf{r}(\mathbf{x}) + g(\langle\alpha\rangle R_{K\Phi}(\mathbf{x}) \\ &+ \langle K_s(\mathbf{x})\rangle R_{\alpha\Phi}(\mathbf{x}) + R_{\alpha K\Phi}(\mathbf{x}))\mathbf{e}_3. \end{aligned} \quad (\text{A10})$$

Appendix B

[46] Expressing equation (A8) in terms of \mathbf{y} , multiplying by $Y'(\mathbf{x})$, and taking conditional ensemble mean gives

$$\begin{aligned} \langle Y'(\mathbf{x})\Phi'(\mathbf{y}) \rangle &= - \int_{\Omega} \langle Y'(\mathbf{x})\nabla_{\mathbf{z}}^T G(\mathbf{z}, \mathbf{y})K'_s(\mathbf{z}) \rangle [\nabla\langle\Phi(\mathbf{z})\rangle + g\langle\alpha\rangle \\ &\cdot \langle\Phi(\mathbf{z})\rangle\mathbf{e}_3] d\Omega - \int_{\Omega} \langle Y'(\mathbf{x})\nabla_{\mathbf{z}}^T G(\mathbf{z}, \mathbf{y}) \rangle \mathbf{r}(\mathbf{z}) d\Omega \\ &- g \int_{\Omega} \langle \alpha'Y'(\mathbf{x})\nabla_{\mathbf{z}}^T G(\mathbf{z}, \mathbf{y})K_s(\mathbf{z}) \rangle \langle\Phi(\mathbf{z})\rangle\mathbf{e}_3 d\Omega \\ &+ g \int_{\Omega} \langle Y'(\mathbf{x})\nabla_{\mathbf{z}}^T G(\mathbf{z}, \mathbf{y}) \rangle (\langle\alpha\rangle R_{K\Phi}(\mathbf{z}) \\ &+ \langle K_s(\mathbf{z})\rangle R_{\alpha\Phi}(\mathbf{z}) + R_{\alpha K\Phi}(\mathbf{z}))\mathbf{e}_3 d\Omega \\ &- \int_{\Gamma_D} \langle Y'(\mathbf{x})H'(\mathbf{z})\nabla_{\mathbf{z}}^T G(\mathbf{z}, \mathbf{y})K_s(\mathbf{z}) \rangle \mathbf{n}(\mathbf{z}) d\Gamma, \end{aligned} \quad (\text{B1})$$

where

$$\begin{aligned} \mathbf{r}(\mathbf{z}) &= -\langle K'_s(\mathbf{z})\nabla\Phi'(\mathbf{z}) \rangle \quad R_{K\Phi}(\mathbf{z}) = \langle K'_s(\mathbf{z})\Phi'(\mathbf{z}) \rangle \\ R_{\alpha\Phi}(\mathbf{z}) &= \langle \alpha'\Phi'(\mathbf{z}) \rangle \quad R_{\alpha K\Phi}(\mathbf{z}) = \langle \alpha'K'(\mathbf{z})\Phi'(\mathbf{z}) \rangle. \end{aligned} \quad (\text{B2})$$

[47] Expanding equation (B1) to second order in σ_Y yields

$$\begin{aligned} C_{Y\Phi}^{(2)}(\mathbf{x}, \mathbf{y}) &= - \int_{\Omega} C_Y(\mathbf{x}, \mathbf{z})\nabla_{\mathbf{z}}^T \langle G^{(0)}(\mathbf{z}, \mathbf{y}) \rangle K_G(\mathbf{z}) \\ &\cdot \left[\nabla\langle\Phi^{(0)}(\mathbf{z})\rangle + g\alpha_G\langle\Phi^{(0)}(\mathbf{z})\rangle\mathbf{e}_3 \right] d\Omega \end{aligned} \quad (\text{B3})$$

from whence

$$\langle \mathbf{K}'_s(\mathbf{x})\Phi'(\mathbf{y}) \rangle^{(2)} = K_G(\mathbf{x})\langle Y'(\mathbf{x})\Phi'(\mathbf{y}) \rangle^{(2)}. \quad (\text{B4})$$

Appendix C

[48] Rewriting equation (8) as

$$\alpha\psi(\mathbf{x}) = \ln[\alpha\Phi(\mathbf{x})] \quad (\text{C1})$$

and expanding yields

$$\begin{aligned} \alpha[\langle\psi(\mathbf{x})\rangle + \psi'(\mathbf{x})] &= \ln \left[\alpha_G \langle\Phi^{(0)}(\mathbf{x})\rangle \right] + \frac{\Phi'(\mathbf{x})}{\langle\Phi^{(0)}(\mathbf{x})\rangle} \\ &+ \frac{\langle\Phi^{(2)}(\mathbf{x})\rangle}{\langle\Phi^{(0)}(\mathbf{x})\rangle} - \frac{1}{2} \frac{\langle\Phi'^2(\mathbf{x})\rangle}{\langle\Phi^{(0)}(\mathbf{x})\rangle^2} + \dots \end{aligned} \quad (\text{C2})$$

[49] The conditional mean of equation (C2) is

$$\begin{aligned} \langle\alpha\rangle\langle\psi(\mathbf{x})\rangle &= \ln \left[\alpha_G \langle\Phi^{(0)}(\mathbf{x})\rangle \right] \\ &+ \frac{\langle\Phi^{(2)}(\mathbf{x})\rangle}{\langle\Phi^{(0)}(\mathbf{x})\rangle} - \frac{1}{2} \frac{\langle\Phi'^2(\mathbf{x})\rangle}{\langle\Phi^{(0)}(\mathbf{x})\rangle^2} + \dots \end{aligned} \quad (\text{C3})$$

Equating terms of same order on the two sides of equation (C3) yields, up to second order in σ_Y ,

$$\langle \psi^{(0)}(\mathbf{x}) \rangle = \frac{1}{\alpha_G} \ln \left[\alpha_G \langle \Phi^{(0)}(\mathbf{x}) \rangle \right] \quad (C4)$$

$$\langle \psi^{(2)}(\mathbf{x}) \rangle = \frac{1}{\alpha_G} \left[\frac{\langle \Phi^{(2)}(\mathbf{x}) \rangle}{\langle \Phi^{(0)}(\mathbf{x}) \rangle} - \frac{1}{2} \frac{C_{\Phi}^{(2)}(\mathbf{x}, \mathbf{x})}{\langle \Phi^{(0)}(\mathbf{x}) \rangle^2} \right]. \quad (C5)$$

Taking the product of equation (C1) with the same expression written in terms of \mathbf{y} gives

$$\alpha^2 \psi(\mathbf{x}) \psi(\mathbf{y}) = \ln[\alpha \Phi(\mathbf{x})] \ln[\alpha \Phi(\mathbf{y})]. \quad (C6)$$

Expanding equation (C6) and taking conditional mean yield

$$\begin{aligned} & \langle \alpha \rangle^2 \langle \psi(\mathbf{x}) \rangle \langle \psi(\mathbf{y}) \rangle + \langle \alpha \rangle^2 C_{\psi}(\mathbf{x}, \mathbf{y}) \\ &= \ln \left[\alpha_G \langle \Phi^{(0)}(\mathbf{x}) \rangle \right] \ln \left[\alpha_G \langle \Phi^{(0)}(\mathbf{y}) \rangle \right] + \frac{\langle \Phi'(\mathbf{x}) \Phi'(\mathbf{y}) \rangle}{\langle \Phi^{(0)}(\mathbf{x}) \rangle \langle \Phi^{(0)}(\mathbf{y}) \rangle} \\ &+ \ln \left[\alpha_G \langle \Phi^{(0)}(\mathbf{x}) \rangle \right] \left[\frac{\langle \Phi^{(2)}(\mathbf{y}) \rangle}{\langle \Phi^{(0)}(\mathbf{y}) \rangle} - \frac{1}{2} \frac{\langle \Phi'^2(\mathbf{y}) \rangle}{\langle \Phi^{(0)}(\mathbf{y}) \rangle^2} \right] \\ &+ \ln \left[\alpha_G \langle \Phi^{(0)}(\mathbf{y}) \rangle \right] \left[\frac{\langle \Phi^{(2)}(\mathbf{x}) \rangle}{\langle \Phi^{(0)}(\mathbf{x}) \rangle} - \frac{1}{2} \frac{\langle \Phi'^2(\mathbf{x}) \rangle}{\langle \Phi^{(0)}(\mathbf{x}) \rangle^2} \right] + \dots \quad (C7) \end{aligned}$$

Equating terms of same order on the two sides of equation (C7) and substituting equations (C4) and (C5) into the result lead directly to equation (48).

[50] **Acknowledgments.** This work was supported in part by the U.S. National Science Foundation under grant EAR-9628133 and by the U.S. Army Research Office under grant DAAD 19-99-1-0251.

References

- Bear, J., *Dynamics of Fluids in Porous Media*, Dover, Mineola, N. Y., 1972.
- Gardner, W. R., Some steady state solutions of unsaturated moisture flow equations with applications to evaporation from a water table, *Soil Sci.*, 85, 228–232, 1958.
- Gómez-Hernández, J. J., A stochastic approach to the simulation of block conductivity fields conditioned upon data measured at a smaller scale, Ph.D. dissertation, Stanford Univ., Stanford, Calif., 1991.
- Guadagnini, A., and S. P. Neuman, Nonlocal and localized analyses of conditional mean steady state flow in bounded, randomly nonuniform domains, 1, Theory and computational approach, *Water Resour. Res.*, 35(10), 2999–3018, 1999a.
- Guadagnini, A., and S. P. Neuman, Nonlocal and localized analyses of conditional mean steady state flow in bounded, randomly nonuniform domains, 2, Computational examples, *Water Resour. Res.*, 35(10), 3019–3039, 1999b.
- Lu, Z., Nonlocal finite element solutions for steady state unsaturated flow in bounded randomly heterogeneous porous media using the Kirchhoff transformation, Ph.D. dissertation, Univ. of Arizona, Tucson, 2000.
- Neuman, S. P., and S. Orr, Prediction of steady state flow in nonuniform geologic media by conditional moments: Exact nonlocal formalism, effective conductivities, and weak approximation, *Water Resour. Res.*, 29(2), 341–364, 1993.
- Neuman, S. P., D. M. Tartakovsky, C. Filippone, O. Amir, and Z. Lu, Deterministic prediction of unsaturated flow in randomly heterogeneous soils under uncertainty without upscaling, in *Proceedings of the International Workshop on Characterization and Measurement of the Hydraulic Properties of Unsaturated Porous Media*, pp. 1351–1365, University of Calif., Riverside, 1999.
- Tartakovsky, D. M., S. P. Neuman, and Z. Lu, Conditional stochastic averaging of steady state unsaturated flow by means of Kirchhoff transformation, *Water Resour. Res.*, 35(3), 731–745, 1999.
- Vogel, L., M. Cislserova, and J. W. Hopmans, Porous media with linearly variable hydraulic properties, *Water Resour. Res.*, 27(10), 2735–2741, 1991.
- Zhang, D., Nonstationary stochastic analysis of transient unsaturated flow in randomly heterogeneous media, *Water Resour. Res.*, 35(4), 1127–1141, 1999.
- Zhang, D., and C. L. Winter, Nonstationary stochastic analysis of steady state flow through variable saturated, heterogeneous media, *Water Resour. Res.*, 34(5), 1091–1100, 1998.
- Zhang, D., T. C. Walstrom, and C. L. Winter, Stochastic analysis of steady state unsaturated flow in heterogeneous media: Comparison of Brooks-Corey and Gardner-Russo models, *Water Resour. Res.*, 34(6), 1437–1449, 1998.
- A. Guadagnini, Dipartimento di Ingegneria Idraulica Ambientale e del Rilevamento, Politecnico di Milano, Piazza L. Da Vinci 32, 20133 Milano, Italy.
- Z. Lu and S. P. Neuman, Department of Hydrology and Water Resources, University of Arizona, Tucson, Arizona 85721, USA. (neuman@hwr.arizona.edu)
- D. M. Tartakovsky, Group CIC-19, MS B256, Los Alamos National Laboratory Los Alamos, New Mexico 87545, USA.